FINAL REPORT

U.S. Department of Energy

Aqueous Electrochemical Mechanisms in Actinide Residue Processing

Principal Investigator: David E. Morris

Institution: Los Alamos National Laboratory

Collaborators:	Carol J. Burns	Los Alamos National Laboratory
	Wayne H. Smith	Los Alamos National Laboratory
	David L. Blanchard, Jr.	Pacific Northwest National Laboratory

Project Number: 59967

Grant Number: [unknown]

Grant Project Officers: Ker Chee Chang

Project Duration: October 1, 1997 through September 30, 2000

Table of Contents

Executive Summary:

Plutonium and uranium residues (e.g., incinerator ash, combustibles, and sand/slag/crucibles) resulting from the purification and processing of nuclear materials constitute an enormous volume of "lean" processing waste and represent a significant fraction of the U. S. Department of Energy's (DOE) legacy waste from fifty years of nuclear weapons production activities. Much of this material is presently in storage at sites throughout the DOE weapons production complex (most notably Rocky Flats, Savannah River and Hanford) awaiting further processing and/or final disposition. The chemical and physical stability of much of this material has been called into question recently by the Defense Nuclear Facility Safety Board (DNFSB) and resulted in the issuance of a mandate by the DNFSB to undertake a program to stabilize these materials. Additional processing of some of these residue waste streams to reduce radionuclide activity levels, matrix volume, or both is a potentially important strategy to achieve both stabilization and volume reduction so that the anticipated geologic repositories will provide adequate storage volume. Mediated electrochemical oxidation and/or reduction processes (MEO/R) are one potential approach to processing of these materials to achieve stabilization/volume reduction. However, the fundamental aspects of this technology as they apply to actinide chemistry are not completely understood. The principal goal of the work described here is to develop a fundamental understanding of the heterogeneous electron transfer thermodynamics and kinetics that lie at the heart of the MEO/R processes for actinide solids and actinide species entrained in or surface-bound to residue substrates. This has been accomplished as described in detail below through spectroscopic characterization of actinide-bearing substrates and electrochemical investigations of electron transfer reactions between uranium- and plutonium- (or surrogates) bearing solids (dispersed actinide solid phases and actinides sorbed to inorganic and organic colloids) and polarizable electrode materials. In general, the actinide solids or substrate-supported species were chosen to represent relevant residue materials (e.g., incinerator ash, sand/slag/crucible, and combustibles).

Sorption reactions were conducted for UO_2^{2+} and Eu^{3+} on SiO_2, TiO_2, and several aluminosilicate clay minerals. The sorption reactions were quantified by standard analytical methods and uptake curves were constructed to assist in identifying the nature

of the sorption mechanism. For some of the actinide/oxide sorption samples a dehydration process was performed to mimic the calcination used to stabilize the actinide-bearing residue materials. Identification of the surface complexes of this actinide and actinide surrogate with these solid substrates was determined by luminescence spectroscopy. Baseline electrochemical studies were conducted to identify the factors in homogeneous solution (identity and nature of the coordinating ligand) that influence the redox energetics and kinetics. Detailed electrochemical studies were conducted on the aqueous suspensions of actinide-bearing oxides prior to and following dehydration and on the sorption reaction supernates. These studies provided a means to assess the effects of surface interactions between the actinide species and the oxide substrates on redox energetics and kinetics.

Highlights of the experimental results include:

- Sorption of Eu^{3+} and UO_2^{2+} to SiO_2, TiO_2, and the clay minerals was extensive in most cases over the pH range from ~ 2 to 6. The surface complexes formed by these metals with the oxide substrates are best described in most cases as inner-sphere with a direct bonding interaction between the metal ion and the surface hydroxyl groups. Dehydration of these metal/oxide substrate sorption samples at ~ 200 °C leads to significant loss of coordinated water from the metal surface complex. The surface complex formed by Eu^{3+} with the clay minerals is not so easily defined. Under high loading conditions for the sodium-saturated clay (SWy-1), the data support an assignment of predominantly an exchange-type complex with the hydrated Eu^{3+} cation occupying sites on the basal planes of the sheet aluminosilicate structure.
- Results from studies of the redox energetics and kinetics for the reaction $UO_2^{2+} + e^- = UO_2^+$ in homogeneous aqueous media containing various complexing ligands reveal an enormous variability in properties. The reduction potential varies by ~ 1V on going from the simple aquated uranyl cation to the carbonate and hydroxide complexes of uranyl and the electron transfer rate constant varies by nearly four orders of magnitude for similar changes in coordination environment. The variation in the energetics can be linked to changes in the basicity of the equatorial coordination sphere, but the origin of the variability in the kinetic properties is less easily identified.

- The electrochemical behavior for the reduction of Eu^{3+} on the fully hydrated oxide substrates (SiO_2 and TiO_2) is not significantly perturbed relative to the behavior in bulk homogeneous solution. This result is consistent with the nature of the surface complex defined by the spectral characterization that suggest a weak inner-sphere surface species with a highly hydrated metal cation. In contrast, if the Eu^{3+}-bearing oxide substrates are first dehydrated before undergoing electrochemical interrogation, the redox properties are substantially modified. The dehydrated surface Eu^{3+} species are easier to reduce than the fully hydrated precursors and the electron-transfer kinetics are more facile. This series of investigations most closely mimics the actual plutonium residue waste stream and suggests that the Pu residues should be quite amenable to MEO/R processing.
- The electrochemical behavior of the UO_2^{2+}-bearing oxide supports is also consistent with expectations based on the characterization of the surface complexation. The stronger surface interactions (relative to the Eu^{3+} species) are manifest in a more negative redox potential vs. the fully aquated UO_2^{2+} cation in homogeneous solution and more sluggish electron-transfer kinetic behavior.
- Overall, these data demonstrate that lower valent actinides (e.g., Pu^{4+}, U^{4+}, etc.) will most likely lend themselves to MEO/R processing schemes to remove them from oxide-like substrates because they will interact less strongly with the substrate and apparently are rendered more intrinsically electrochemically reactive as a result of dehydration (e.g., from calcination).

The efforts from this project have and/or will lead to numerous presentations at national meetings and several peer-reviewed publications. In addition, this project actively engaged two undergraduate students. One of the students parlayed her experience on this project into an undergraduate scholarship under the auspices of the U. S. Department of Energy 1999-2000 DOE Environmental Management Scholarship Program Hispanic Scholarship Fund and the other is using her research results as the basis for her senior chemistry thesis project at FurmanUniversity.

Research Objectives:

Background

Plutonium and uranium residues (e.g., incinerator ash, combustibles, and sand/slag/crucibles) resulting from the purification and processing of nuclear materials constitute an enormous volume of "lean" processing waste and represent a significant fraction of the U. S. Department of Energy's (DOE) legacy waste from fifty years of nuclear weapons production activities. Much of this material is presently in storage at sites throughout the DOE weapons production complex (most notably Rocky Flats, Savannah River and Hanford) awaiting further processing and/or final disposition. The chemical and physical stability of much of this material has been called into question recently by the Defense Nuclear Facility Safety Board (DNFSB) and resulted in the issuance of a mandate by the DNFSB to undertake a program to stabilize these materials [1]. The ultimate disposition for much of these materials is anticipated to be geologic repositories such as the proposed Waste Isolation Pilot Plant in New Mexico. However, in light of the mandate to stabilize existing residues and the probable concomitant increase in the volume of material to be disposed as a result of stabilization (e.g., from repackaging at lower residue densities), the projected storage volume for these wastes within anticipated geologic repositories will likely be exceeded simply to handle existing wastes.

Additional processing of some of these residue waste streams to reduce radionuclide activity levels, matrix volume, or both is a potentially important strategy to achieve both stabilization and volume reduction so that the anticipated geologic repositories will provide adequate storage volume. In general, the plutonium and uranium that remains in solid residue materials exists in a very stable chemical form (e.g., as binary oxides), and the options available to remove the actinides are limited. However, there have been some demonstrated successes in this vain using aqueous phase electrochemical methods such as the Catalyzed Electrochemical Plutonium Oxide Dissolution (CEPOD) process pioneered by workers at Pacific Northwest National Laboratory in the mid-1970s [2]. The basis for most of these mediated electrochemical oxidation / reduction (MEO/R) processes is the generation of a dissolved electrochemical catalyst, such as Ag^{2+}, which is capable of oxidizing or reducing solid-phase actinide species or actinide sorbates via

heterogeneous electron transfer to oxidation states that have significantly greater solubilities (e.g., $PuO_{2(s)}$ to $PuO_2^{2+}{}_{(dissolved)}$). The solubilized actinide can then be recovered by ion exchange or other mechanisms.

These aqueous electrochemical methods for residue treatment have been considered in many of the "trade studies" to evaluate options for stabilization of the various categories of residue materials. While some concerns generally arise (e.g., large secondary waste volumes could results since the process stream normally goes through anion exchange or precipitation steps to remove the actinide), the real utility and versatility of these methods should not be overlooked. They are low temperature, ambient pressure processes that operate in a non-corrosive environment. In principle, they can be designed to be highly selective for the actinides (i.e., no substrate degradation occurs), they can be utilized for many categories of residue materials with little or no modification in hardware or operating conditions, and they can conceivably be engineered to minimize secondary waste stream volume. However, some fundamental questions remain concerning the mechanisms through which these processes act, and how the processes might be optimized to maximize efficiency while minimizing secondary waste. In addition, given the success achieved to date on the limited set of residues, further research is merited to extend the range of applicability of these electrochemical methods to other residue and waste streams.

The principal goal of the work described here is to develop a fundamental understanding of the heterogeneous electron transfer thermodynamics and kinetics that lie at the heart of the MEO/R processes for actinide solids and actinide species entrained in or surface-bound to residue substrates. This has been accomplished as described in detail below through spectroscopic characterization of actinide-bearing substrates and electrochemical investigations of electron transfer reactions between uranium- and plutonium- (or surrogates) bearing solids (dispersed actinide solid phases and actinides sorbed to inorganic and organic colloids) and polarizable electrode materials. In general, the actinide solids or substrate-supported species were chosen to represent relevant residue materials (e.g., incinerator ash, sand/slag/crucible, and combustibles).

Significance of Project to EMSP

A detailed accounting of all the actinide-bearing residue materials within the DOE complex is not readily available, and descriptions and nomenclature for these materials tend to vary from site to site. However, the Rocky Flats Environmental Technology Site (RFETS) appears to have the greatest amount of residue material in storage, and their material is reasonably representative of the residue material in storage at other sites including Los Alamos, Hanford, and Savannah River. Data obtained from the Los Alamos Technical Office at RFETS show that there is as much as 100 metric tons (bulk wt.) of residue materials containing significant amounts of plutonium. Important plutonium residue classes at Rocky Flats include graphite, pyrochemical salts, combustibles, incinerator ash, ceramic crucibles, plastic filters, and sand/slag/crucible. Each of these individual classes is reported to have in excess of 5 metric tons of material. Similar waste-stream descriptions and quantities of material pertain for uranium-bearing residues.

For the specific residue classes cited above from RFETS, many are potential candidates for actinide removal by MEO/R - based processes. In particular, workers at Pacific Northwest National Laboratory and in Europe have already demonstrated [2,3] that incinerator ash, ceramic crucibles, sand, and related matrices can be successfully treated with oxidative catalysts to remove plutonium to low levels. MEO/R - based processing of many sub-classes of combustible materials and plastic filters also offers significant promise and provides a potentially important alternative to other stabilization and/or treatment strategies. In particular, the MEO/R approaches can be tailored so that they will not degrade the principally organic-based substrates in these combustible materials. Thus, the majority of the residue volume, which is comprised of the organic substrate, will be simply decontaminated for subsequent disposal as a low-level waste.

Additional areas in which MEO/R processes and or MEO/R-based mechanistic insights might make a significant contribution are the stabilization and stability assessment for spent nuclear fuels and ceramic and glass waste forms. Redox-based degradation mechanisms (e.g., corrosion) for all three categories of materials are certain to be important contributors to overall stability. While we did not conduct experiments directly on these materials as part of the scope of the present effort, our MEO/R

investigations provide a basis for extrapolation to these other materials, and they establish the appropriate experimental protocols for direct investigations on spent fuels and waste forms at a future time.

The ultimate goal of this work is to enable the development of new, more efficient (re)processing technologies based on aqueous phase electrochemical approaches that can be implemented for the stabilization and volume reduction of existing plutonium- and uranium-bearing residue materials. The ultimate disposition of these materials represents an enormous financial liability to the US taxpayers, and is a significant environmental concern to the public. If successful treatment schemes can be devised to reduce the volume of waste that must be disposed and to make the waste that is disposed more stable, the DOE will realize important cost savings and enhanced credibility with the public.

Methods and Results:

Experimental Details

Materials

The metal oxide substrates were obtained from Degussa Corp. The SiO_2 is Aerosil 200. It is amorphous with a reported N_2 BET surface area of ~ 200 m^2/g and an average particle size of ~ 25 nm. The TiO_2 is Titandioxid P25. It is a mixed phase comprised of ~ 70 % anatase and 30 % rutile with a BET surface area of ~ 50 m^2/g and an average particle size of ~ 20 nm. The pH at the point of zero surface charge (pH_{pzc}) for amorphous SiO_2 is typically 2-3 while that for TiO_2 is typically ~ 6 [4]. The clay minerals were obtained from the University of Missouri Source Clay Repository [Na^+- (SWy-1) and Ca^{2+}- (SAz-1) saturated smectites] or were provided from the DOE Subsurface Science Program collection [Na+ - saturated isolates from Kentucky (LK-1) and Washington (R-9)] maintained at Pacific Northwest National Laboratory. Details concerning the chemical and physical properties of these clay minerals are available elsewhere [5,6]. The Eu^{3+} source was $Eu(NO_3)_3 \bullet 6H_2O$ from Aldrich and the UO_2^{2+} source was $UO_2(NO_3)_2 \bullet 6H_2O$ from Strem. The substrates and the sorbates were used without further purification. All other reagents (HNO_3, NaOH, $NaNO_3$, and ligands) were ACS reagent grade.

Instrumentation

Quantitative evaluation of the uptake of sorbate onto the metal-oxide and clay mineral substrates was performed by inductively coupled plasma atomic emission spectroscopic analysis (Varian Model Liberty 220) of the supernates from the batch reactions under the assumption of mass balance between the solid and supernate phases (i.e., negligible container losses). This assumption has been verified in our labs as described elsewhere [7]. The molecular luminescence investigations of the reaction supernates and the solids were carried out on a SPEX Industries Fluorolog 2 System consisting of a Model 1681 single-stage 0.22 m excitation monochromator and a Model 1680 two-stage 0.22 m emission monochromator with a thermoelectrically-cooled Hamamatsu Model R928 photomultiplier tube with photon-counting electronics. Continuous excitation was provided by a high-pressure 450 W Xe arc lamp and pulsed (time-resolved) excitation was provided by a Model 1934 Phosphorimeter attachment. Spectra reported here have not been corrected for monochromator or detector responses. Wet solids were contained in standard-bore borosilicate glass NMR tubes, dry solids were contained in borosilicate capillary tubes, and supernates were contained in standard fluorescence cuvettes for the spectral analyses. Most samples were examined at room temperature, but some uranyl samples were also run at ~ 77 °K in an insertion dewar. Electrochemical investigations were conducted using a Princeton Applied Research Corporation Model 263 Potentiostat with a Model 303A Static Mercury Drop Electrode under computer control using Model 270 software. Solutions were purged with dry nitrogen prior to the collection of data.

Methods & Protocols

Our efforts have focused on model systems prepared to mimic the salient characteristics of incinerator ash (substrate composition, disposition of the actinides, etc.) while providing both electrochemical and spectroscopic properties to enable adequate characterization of local environments and redox properties. In particular, we have chosen colloidal SiO_2 and TiO_2 as the substrates since these have been identified as significant components in real ash samples [8] and yield stable aqueous suspensions at high solids concentrations. They have also been shown to sorb actinides from aqueous

solutions. Unlike colloidal metal oxides which provide only external surface sorption sites, colloidal smectitic clay minerals possess intrinsically internal sorption sites that exist between the basal planes of the tetrahedral silica sheets. These sites are created as a consequence of the isomorphous substitution of framework metals (e.g., Al^{3+} for Si^{4+} in the tetrahedral sheets) that leads to net negative structural charge which must be compensated by hydrated cations at the basal planes. These samples provide a means of investigating redox energetics for this distinctly different (internal) structural site similar to what might be encountered for actinides entrained in metal oxides. These materials also form stable suspensions at high solids concentrations.

The sorbates include UO_2^{2+} and Eu^{3+} (as an actinide surrogate). These metals possess one or more redox couples in aqueous solution and they have spectroscopic properties that are sensitive to speciation, surface complexation, and changes therein. These metals also have excellent luminescence characteristics that provide for exceptional sensitivity when probing speciation. In particular, the luminescence characteristics of Eu^{3+} have been extensively exploited for investigations of the coordination environment surrounding this metal ion in chemical, biochemical, and, more recently geochemical systems [9]. There have been surprisingly few reports of the use of Eu^{3+} luminescence to probe surface complexation processes. However, it is ideally suited for this purpose as well because it is highly sensitive in both an analytical sense and with respect to differentiating chemical environments. The most salient features of Eu^{3+} luminescence from which coordination environment information is deduced are the intensity in the "hypersensitive" transition ($^5D_0$ to $^7F_2$ at ~ 16,200 cm^{-1}) relative to that in the $^5D_0$ to $^7F_1$ transition at ~ 16,860 cm^{-1} and the luminescence lifetime. The former property is a reflection of the local symmetry around the ion [10] and the latter changes in response to changes in the number and type of coordinating molecules. Specifically, the lifetime has been shown to correlate with the number of coordinated water molecules [11], and a simple formula has been derived [$n_{H2O} = (1070/\tau_m)-0.62$ where τ_m is the measured lifetime in microseconds] to estimate this [12].

Sorption Reactions on Metal Oxides

The batch sorption reactions with SiO_2 and TiO_2 were performed on solid suspensions that were pre-equilibrated for 24 - 48 hrs in deionized water or ~ 0.1 M $NaNO_3$ solution at the native pH of the suspension. The solid concentration in the suspension was ~ 12-24 g/L for the Eu^{3+} samples and ~ 7-11 g/L for the UO_2^{2+} samples. The sorbate was introduced into the pre-equilibrated suspension as either a solid aliquot of the nitrate salt or a small volume of concentrated spike solution to give a final sorbate concentration of 3 - 8 mM for Eu^{3+} samples and 0.2 - 0.4 mM for UO_2^{2+} samples. The pH of the suspension was then adjusted to the target value between pH 2 and 6. The sorption reactions were allowed to equilibrate for 36 - 48 hrs while undergoing end-over-end rotation. The UO_2^{2+} / TiO_2 suspensions were covered with Al foil prior to introduction of the uranyl spike and for the duration of the equilibration time to prevent photochemical reduction/ surface precipitation of the uranium [13]. The equilibrated suspensions were centrifuged to effect phase separation. The supernates were decanted and retained for analysis. Some of the solid phase was dehydrated in a convection oven at ~ 200 °C for 12-24 hrs to partially simulate the effects of residue incineration. The remainder of the solid phase was kept moist for spectroscopic interrogation and electrochemical studies.

Sorption Reactions on Clay Minerals

The batch sorption reactions with the clay minerals were performed on solid suspensions (~ 10 g/L) that were pre-equilibrated for 24 - 48 hrs in 0.001 M $NaNO_3$ (SWy-1, LK-1, and R-9) or 0.0005 M $Ca(NO_3)_2$ (SAz-1). The equilibrated samples were adjusted to target pH values of ~4 and ~ 5 and spiked with standard Eu^{3+} solutions to give an initial solution concentration of 10, 50, 100 and 200 ppm. The samples were allowed to re-equilibrate in the presence of the Eu^{3+} for 24 - 48 hrs at the target pH values while undergoing end-over-end rotation. The pH was adjusted as needed to maintain a value close to the target. The equilibrated suspensions were centrifuged to effect phase separation. The supernates were decanted and retained for analysis.

Results and Discussion

Sorption Reactions on Metal Oxides

The strategies for the batch sorption experiments were based on published reports for UO_2^{2+} sorption on SiO_2 [6] and Co^{2+} sorption on TiO_2 [14]. Specifically, these reports were used to guide in the selection of solid substrate concentration ranges (and therefore site densities) relative to the sorbate concentrations in solution. The oxide substrates used in these reports are not identical to those used here. However, these published reports were used to estimate surface sorption site densities for the materials used in this report as follows; 0.14 mmol sites /g solid for SiO_2 and 0.25 mmol sites / g solid for TiO_2. The aim was to have high sorbate concentrations on the solids at equilibrium to facilitate the subsequent electrochemical and spectroscopic investigations, yet not exceed the total sorption site density on the solids and risk introducing complicating sorption mechanisms like surface precipitation.

An additional important consideration was the solution speciation of the sorbate cations vs. pH in the sorption reactions. Uranyl ion is a much stronger Lewis acid than Eu^{3+}. Thus, it is more susceptible to formation of insoluble hydroxide species at lower pH for any given concentration. For this reason, the total $[UO_2^{2+}]$ in the reactions was kept about a factor or 10 lower than the corresponding $[Eu^{3+}]$. Calculations using HYDRAQL [15] and the NEA/OECD database [16] for uranyl indicated that precipitation of uranyl hydroxide phases should not be important under the conditions applied here. Finally, sorption reactions were run with and without added $NaNO_3$ electrolyte (0.08 M) to assist in determining whether the sorption reactions were inner- vs. outer-sphere in nature. High electrolyte concentrations are known to reduce sorption by outer sphere mechanisms via mass-balance driven competition for these electrostatically governed sites [4].

Typical uptake curves for Eu^{3+} and UO_2^{2+} on the solid substrates are shown in Figure 1. All systems show the onset of a sorption "edge" typical of metal ion sorption onto oxide phases [4, 17]. Note that UO_2^{2+} uptake is significantly greater on all solids than that for Eu^{3+}. In addition, the sorption edge occurs at much higher pH for the Eu^{3+} samples. This is consistent with the much higher metal ion concentration in these solutions than in the corresponding UO_2^{2+} systems, but it also likely reflects important

differences in the strength of surface binding of Eu^{3+} vs. UO_2^{2+} as well as differences in the hydrolysis properties of these two cations. The edge for TiO_2 sorption occurs at lower pH than that for SiO_2 in all systems. This is consistent with results obtained for Co^{2+} sorption on these same substrates [17]. Although the pH_{pzc} for SiO_2 is lower than that for TiO_2, the reversal in the pH of the sorption edge is interpreted to indicate stronger binding of the metal ion to titania than to silica [17]. There is no discernible ionic-

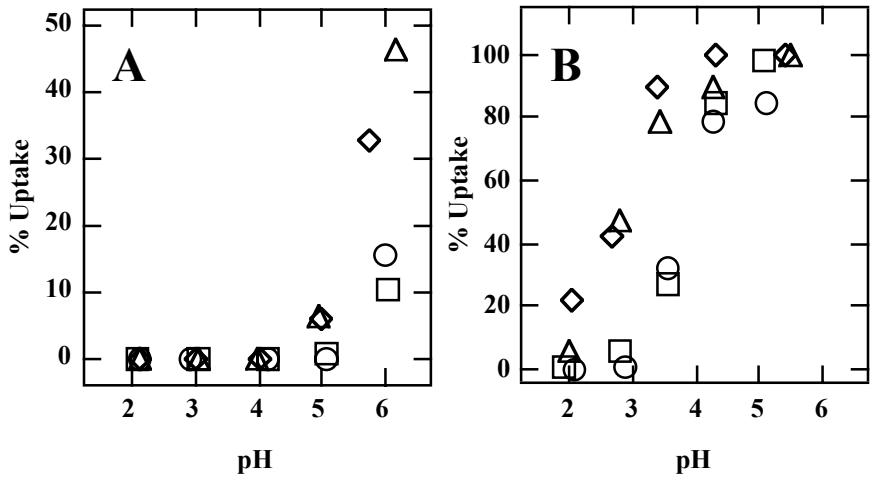

Figure 1. Sorption data for (A) ~ 3 mM Eu^{3+} and (B) ~ 0.2 mM UO_2^{2+} on oxide substrates. (O) SiO_2. (SQUARES) SiO_2 with 0.08 M $NaNO_3$. (Δ) TiO_2. (◊) TiO_2 with 0.08 M $NaNO_3$. Solid concentrations are ~ 12 g/L for Eu^{3+} and ~ 7.5 g/L for UO_2^{2+} samples.

strength dependence in the UO_2^{2+} sorption data. This, coupled with the typical sorption-edge behavior indicates that the uranyl species are forming inner-sphere surface complexes on both substrates. The Eu^{3+} sorption data appear to have a very slight ionic-strength dependence, with the sorption suppressed somewhat at the higher ionic strength. However, the effect is minimal and only observed at the highest pH. This observation, coupled with the spectroscopic data described below, are more consistent with an inner-sphere description for the Eu^{3+} sorption complexes on both substrates as well.

Overall, these sorption data are consistent with those reported for related systems in other recent studies. For example, the sorption of Eu^{3+} and other trivalent lanthanides on silica [18] and the iron-oxide hematite [19] was interpreted to occur via an inner-sphere mechanism. Notably, in the SiO_2 sorption study the sorption edge at the highest Ln^{3+} concentration (0.1 mM) was at about the same pH as the edge observed in the present study (Figure 1A). Uranyl sorption has also been reported on SiO_2 [20-22] and TiO_2 [23],

and in all cases the sorption mechanisms has been described as inner-sphere in nature. Thermodynamic modeling of sorption data has also been carried out in some of these previous studies, and surface binding constants have been published for some trivalent lanthanide ions on SiO_2 [18] and for UO_2^{2+} on SiO_2 [21].

Sorption Reactions on Clay Minerals

One of the key questions in the studies of the clay minerals was whether selective populations of basal-plane exchange sites could be prepared by suitable manipulation of the solution condition under which the samples were prepared. The conditions that favor the creation of exchange site populations have been enumerated by Zachara and co-workers [6, 21]. They include low concentrations of other exchangeable cations typically used to adjust the ionic strength of the reactions (e.g., salts of alkali and alkaline earth metals) to suppress mass action effects, and low pH to inhibit sorption of the metals to the external amphoteric oxygen sites on the crystallite surfaces and edges. There should also be a strong driving force for incorporation of trivalent metal ions into exchange sites because of the favorable electrostatic interactions between the structural negative charge and the large positive scalar charge of the trivalent ion. This effect has been utilized previously with La^{3+} exchange to quantify the concentration of exchange sites in these materials.

The sorption data for Eu^{3+} on these smectitic samples are summarized in Fig. 2. For the two soil isolate samples (LK-1 from Kentucky and R-9 from Washington) the uptake at both pH 4 and 5 is essentially quantitative over the entire range of Eu^{3+} solution concentrations investigated. For the reference clay sample from Wyoming (SWy-1) the uptake is quantitative at pH 4, but there is some significant diminution in uptake at pH 5. For the reference clay mineral from Arizona (SAz-1) there was no measurable uptake (based on ICP analysis) at either pH even for the lowest Eu^{3+} solution concentration. (However, spectral data presented below demonstrate that at least trace amounts of Eu^{3+} were taken up by this clay sample.) The lack of a significant sorption process for Eu^{3+} on SAz-1 is not too surprising since this clay mineral already incorporates the divalent cation, Ca^{2+}, into the exchange sites. Thus, a strong electrostatic interaction already

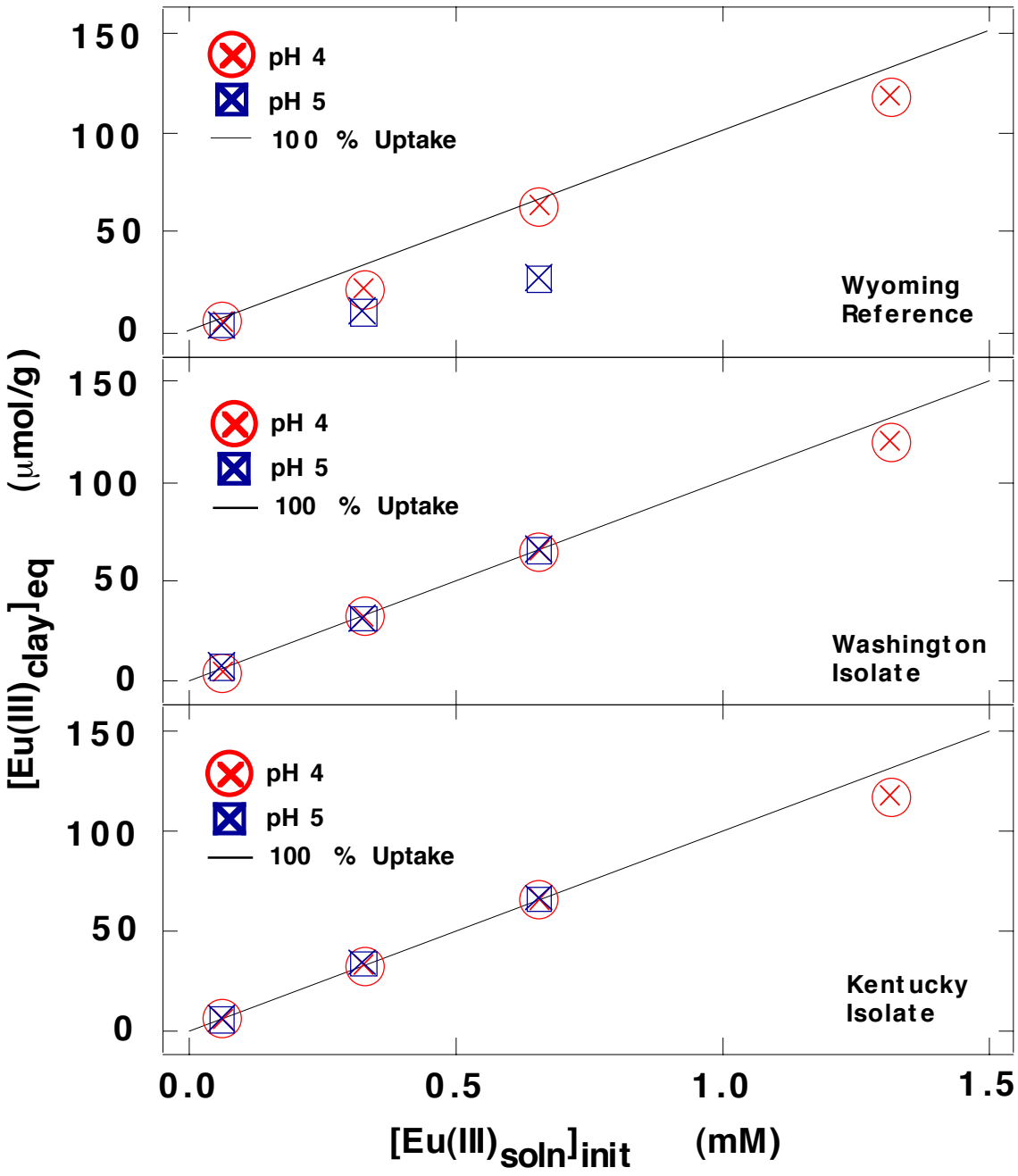

Figure 2. Sorption isotherm data for Eu^{3+} on smectitic clay minerals from ~ 1 mM $NaNO_3$ supporting electrolyte solutions. Solid concentrations are ~ 10 g/L. Solid lines correspond to theoretical maximum uptake.

exists, and it appears that this cannot be overcome to a significant extent with Eu^{3+} at the concentration employed. However, the decrease in the uptake of Eu^{3+} for the SWy-1 sample (a Na^+ - exchanged material) at pH 5 relative to pH 4 is puzzling.

The sorption of aqueous UO_2^{2+} species on these clay minerals has been described in detail [6, 21]. Under conditions similar to those employed here for Eu^{3+} sorption, the uranyl sorption is extensive and the surface complexation is comprised of principally exchange-site complexes at pH 4 and a mixture of exchange-site and inner-sphere edge-site complexes at pH 5.

Characterization of Surface Complexation on Metal Oxides

Representative emission spectral data for Eu^{3+} in the sorption reaction supernates and on the wet SiO_2 and TiO_2 solid phases are shown in Figure 3. These spectra have all been normalized to facilitate comparisons, but the unnormalized intensities track the concentrations determined by ICP/AES (Figure 1). Notably, although there is no analytically measurable uptake at the lower pH values, it is still possible to measure an Eu^{3+} luminescence spectrum on the solids for both SiO_2 and TiO_2 attesting to the sensitivity of this method to track surface complexation. (Samples prepared in other experiments at much lower initial $[Eu^{3+}]$ values and characterized by ICP/AES did show micromolar surface concentrations of Eu on both substrates consistent with the luminescence result here and previous batch sorption studies [18, 19].)

The spectra for the reaction supernate in the SiO_2 reactions are invariant over the entire pH range and look identical to that of the pH 4 standard solution (Figure 3A). This confirms that there is not a significant change in the solution speciation for Eu^{3+} over the entire pH range in these equilibrium solutions. This observation is consistent with the speciation data reported recently (albeit presumably at lower $[Eu^{3+}]_{tot}$) that indicates that the initial hydrolysis and carbonate complexes for Eu^{3+} solutions in equilibrium with atmospheric CO_2 (as in the present study) do not contribute significantly to the speciation below ~ pH 6 [19]. Thus, the fully aquated Eu^{3+} cation is the dominant species in these equilibrium supernates. A similar situation exists for the supernates from the TiO_2 reactions at all pH values except pH 6.0 (Figure 3C). For this latter supernate, the spectrum shows a much greater intensity contribution from the hypersensitive transition indicating some change in solution speciation. This change could reflect contributions

from hydrolysis and/or carbonate species, but this seems unlikely since such species were not observed in the SiO_2 supernates, and the equilibrium Eu^{3+} concentration in the TiO_2

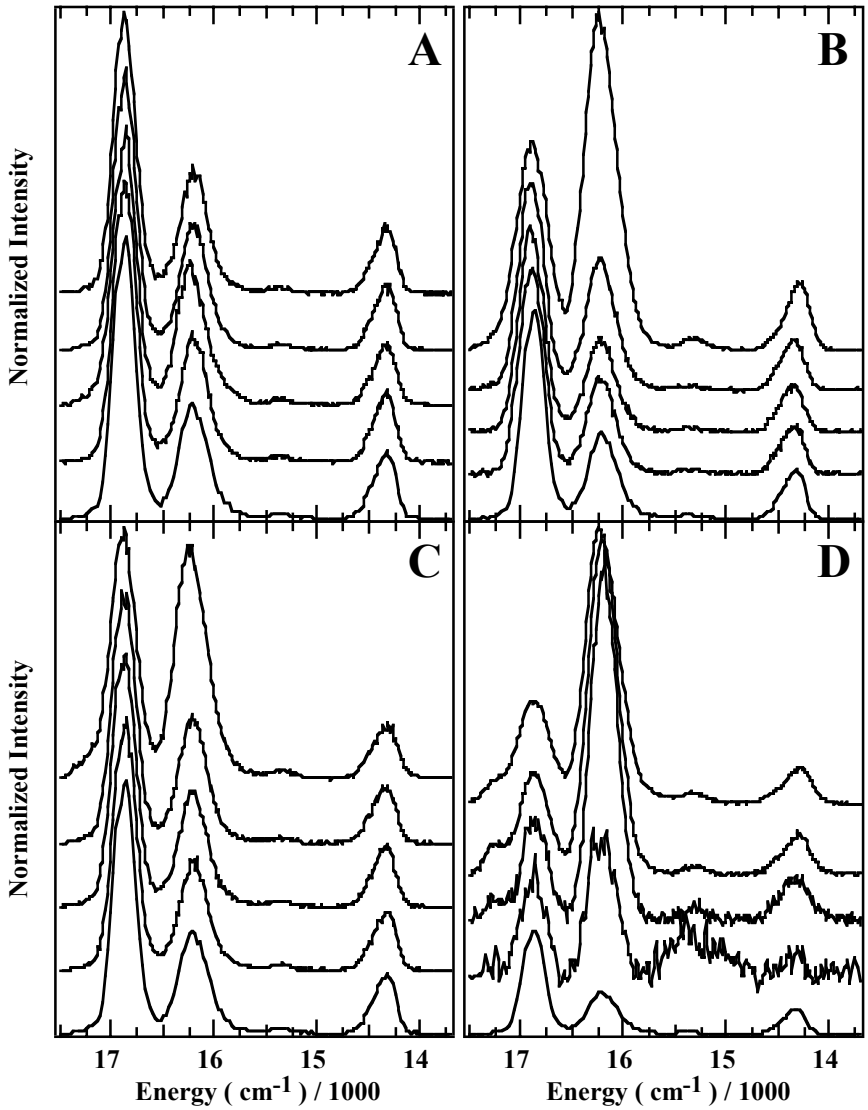

Figure 3. Eu^{3+} luminescence spectra from samples prepared with ~ 6 mM Eu^{3+} and 24 g/L of solid. (A) Supernate from SiO_2 sample. (B) Wet SiO_2 solid. (C) Supernate from TiO_2 sample. (D) Wet TiO_2 solid. All spectra have been normalized to the intensity in the band at 16,860 cm^{-1}. For all panels the order of the spectra from bottom to top is: 5 mM standard solution at pH 4, pH 3.0 sample, pH 4.0 sample, pH 5.0 sample, and pH 6.0 sample. Spectra were obtained with 393 nm pulsed excitation and gated detection using a 50 microsecond delay.

supernates is lower than in the SiO_2 supernates. In addition, the hypersensitive band does not have the general characteristics (splitting into two distinct bands and much greater

intensity relative to the 16,860 cm^{-1} band) reported for carbonate species [24]. The ICP analyses of these supernates did reveal some soluble Ti species from substrate dissolution; more so than Si species at comparable solid concentrations and pH. Perhaps the soluble Ti species are anionic titanates that can interact with the Eu^{3+} cation to lower the local symmetry and thereby give rise to increased intensity in the hypersensitive band.

The spectra for Eu^{3+} on the surface of SiO_2 (Figure 3B) are similar to those seen in the supernate for the lower pH values (2.0 to 4.0) suggesting that the structure of the surface complex is only minimally perturbed from the aquated cation (i.e., more like an outer-sphere complex). However, for the pH 5.0 and 6.0 samples the intensity in the hypersensitive transition increases steadily relative to that in the 16860 cm^{-1} band. The intensity ratio increases from ~ 0.5 at pH 2.0 - 4.0, to ~ 0.7 at pH 5.0, to ~ 1.7 at pH 6.0. This change reflects a much stronger interaction between the Eu^{3+} species and the surface that lowers the symmetry of the coordination environment around the Eu^{3+} cation relative to the aquated species, and likely signals the onset of a true inner-sphere complex. Note that this change takes place within the same pH interval that the uptake increases significantly (Figure 1A) and the system shows the appearance of a classical metal-oxide sorption edge. The emission lifetime data also support the conclusion of a change in surface speciation in the higher pH interval. Notably, the emission decay curves for all Eu^{3+} sorption samples were adequately analyzed using only a single exponential function. This indicates that a single surface species dominates the surface population at any given pH value. The measured lifetime for the wet SiO_2 solids remains constant from pH 2.0 through 5.0 (τ_{ave} = 111±1 μs) but increases to 169 μs at pH 6.0. The former value agrees very well with the value measured for the 5 mM pH 4.0 standard (112 μs). Using the formula cited above [12], the short lifetime which dominates for the low pH surface species corresponds to 9.0 coordinated water molecules while the long lifetime seen in the pH 6.0 solid sample corresponds to 5.7 coordinated waters. Again, these data are consistent with a transition from a fully aquated outer-sphere complex to an inner-sphere complex having lower site symmetry and fewer coordinated waters. Interestingly, previous reports of Ln^{3+} sorption on SiO_2 [18] and iron oxides [19], while proposing inner-sphere complexation mechanisms, do not consider displacement of coordinated water in concert with this process. However, the loss of coordinated water (as

demonstrated by the lifetime data reported here) must accompany the formation of inner-sphere bonds with the surface hydroxyl groups.

For the Eu^{3+} - laden TiO_2 wet solids the luminescence spectra show an even greater perturbation relative to the supernate spectral data. In this system, even at the lowest pH (2.0) the intensity in the hypersensitive transition exceeds that in the 16,860 cm^{-1} band (data at pH 2.0 are not included in Figure 3 for clarity sake). This intensity ratio increases with increasing pH to an approximately constant value in the pH 4.0 – 6.0 samples of 2.5. This perturbation in local symmetry clearly suggests that the surface interaction between Eu^{3+} and the TiO_2 surface sites is much greater, particularly at the lower pH values than is observed in the SiO_2 system. Other metal cation sorbates are also found to interact more strongly with transition-metal oxide substrates than with SiO_2 and its polymorphs [4]. The emission lifetime data for the Eu^{3+} / TiO_2 samples are also consistent with a stronger surface interaction. The measured lifetimes range from 130 μs in the pH 4 solid (the emission was too weak to collect lifetime data for the lower pH samples), to 200 μs in the pH 5 solid, to 220 μs in the pH 6 solid. The calculated number of coordinated water molecules corresponding to these lifetimes are: 7.6 (pH 4), 4.7 (pH 5), and 4.2 (pH 6). Thus, the prediction is that more than half the original coordinated waters have been lost in forming the surface complex of Eu^{3+} with TiO_2 at the higher pH values.

For the Eu^{3+} - substrate samples that were dehydrated at 200 °C, the luminescence data (Figure 4) indicate that the heat treatment has a leveling effect on the surface speciation. That is, the variability observed in the spectra versus pH for the wet samples is essentially gone. The data for dehydrated samples do reflect significant perturbations in the surface complexation, even relative to that seen at the highest pH value for the wet solids. Note that the intensity ratio of the hypersensitive band to the 16,860 cm^{-1} band is greater still for these dehydrated samples than for the pH 6.0 wet solids for both SiO_2 and TiO_2. Consistent with observations from the wet solid data, this perturbation is also greater in the TiO_2 samples than the SiO_2 samples. As expected, the lifetime data from these dehydrated samples also reveal more substantial losses of coordinated H_2O than in the wet solids. However, it is interesting that for the dehydrated samples the Eu^{3+} appears to lose more water on dehydration on the SiO_2 surface than on the TiO_2 surface. The

measured lifetimes range smoothly from 225 μs (4.1 waters) at pH 2.0 to 340 μs (2.5 waters) at pH 6.0 on SiO_2 whereas the range is only 220 μs (4.2 waters) to 280 μs (3.2 waters) on TiO_2.

The luminescence characteristics of the UO_2^{2+} ion have also made this an excellent chromophore for probing speciation in solution and on surfaces. There have been numerous recent reports on uranyl emission as a probe for speciation in groundwaters [25, 26] and on environmentally relevant substrates [7, 22, 26-29]. The way in which speciation information becomes encoded in the spectral response of the uranyl ion is much more complex than in the case of Eu^{3+}. For systems containing the uranyl

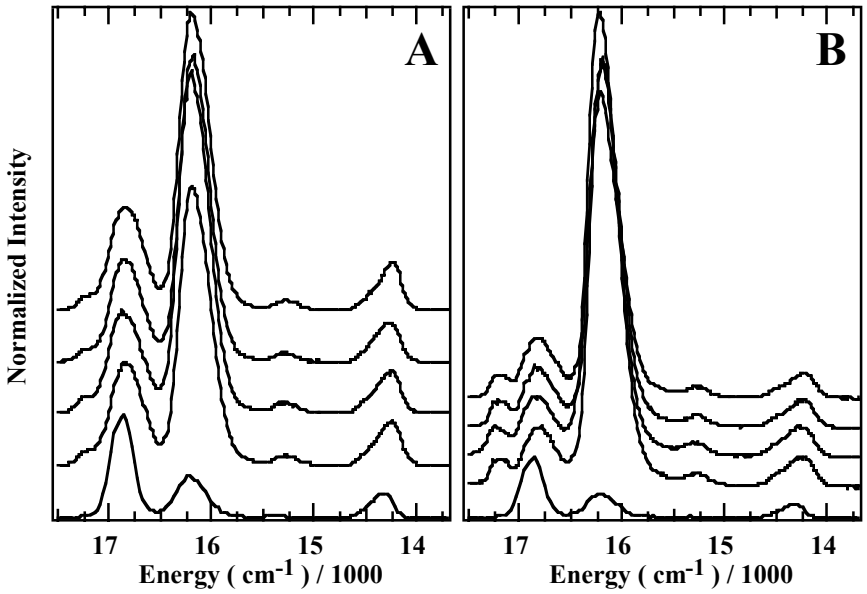

Figure 4. Eu^{3+} luminescence spectra from samples prepared with ~ 6 mM Eu^{3+} and 24 g/L of solid. (A) Dehydrated SiO_2 solid. (B) Dehydrated TiO_2 solid. The order of the spectra from bottom to top in both panels is: 5 mM standard solution at pH 4, pH 3.0 sample, pH 4.0 sample, pH 5.0 sample, and pH 6.0 sample. Spectra were obtained with 393 nm pulsed excitation and gated detection using a 50 microsecond delay. All spectra have been normalized to unit intensity in the band at 16,860 cm^{-1}.

moiety the structural information can only be inferred based on trends in spectroscopic responses. Nonetheless, significant progress has been made in this area in relation to problems in environmental and surface complexation chemistries. With respect to the

present study, uranyl poses several additional challenges. First, the onset of hydrolysis for uranyl occurs at low pH, even for the relatively dilute solutions used to prepare the sorption samples, and there are a large number of hydrolytic species possible in the pH range 2 to 6. This has the practical consequence of making it fruitless to compare in detail the supernate spectra from one pH to another given the changes in $[UO_2^{2+}]_{tot}$ in these solutions. Second, uranyl is photochemically very active and interacts with TiO_2 via energy and electron transfer mechanisms [13] that lead to substantially quenching of the luminescence signal. Thus, characterization of the uranyl surface complexes on TiO_2 by luminescence, if possible, may require additional steps to overcome the quenching (e.g., low temperatures).

Typical luminescence data obtained for UO_2^{2+} on SiO_2 and TiO_2 substrates are shown in Figure 5. These spectra have also been normalized to facilitate comparison. However, here too, the raw intensities track the concentration trends exhibited in the batch sorption data (Figure 1B). The spectra obtained for the wet SiO_2 solid samples (Figure 5A) show very little variation with pH. There is only a slight increase in the intensity of the shoulder at ~ 18,300 cm^{-1} with increasing pH which signifies a very minor contribution from an additional species that grows in at the higher pH. For comparison, the spectrum of the pH 2.1 supernate has been included. This solution is dominated by the fully aquated UO_2^{2+} monomer species, and the spectrum reflects this dominant population. The spectral benchmark for both hydrolysis [24] and inner-sphere surface complexation [7] in uranyl systems is a shift to lower energy (red shift) in the spectral band relative to that of the fully aquated monomer. This behavior is clearly observed for these wet SiO_2 samples indicating that the UO_2^{2+} is forming inner-sphere surface complexes. However, the essentially constant spectral behavior over the pH range investigated suggests that a single uranyl surface complex is dominating these samples. This observation is in agreement with recently published work on batch sorption and thermodynamic modeling of uranyl on SiO_2 which suggest a single dominant uranyl surface complex over the pH range investigated here [6]. The luminescence lifetime data for these wet solid samples support the dominance of a single inner-sphere surface complex; only a single lifetime is observed in the decay data, and it remains constant within experimental error at 238 ± 14 μs. (Emission from the pH 2.1 sample was too weak to obtain a lifetime.)

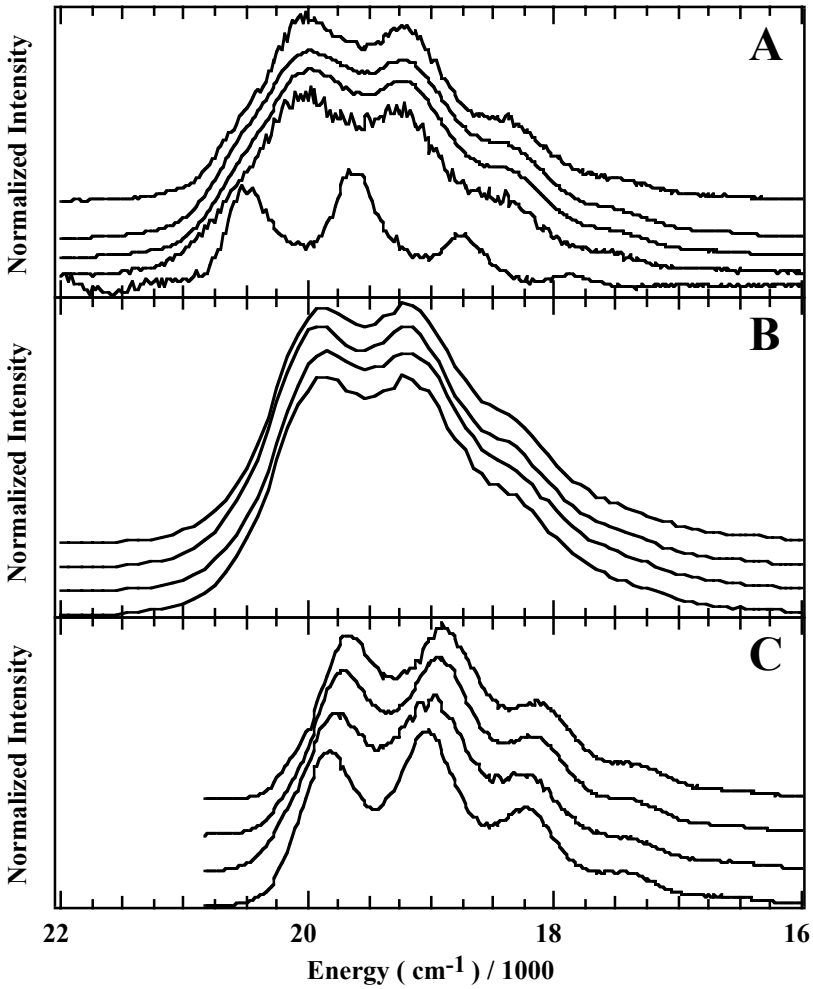

Figure 5. UO_2^{2+} luminescence spectra for samples prepared with ~ 0.3 mM UO_2^{2+} and ~ 12 g/L of solid. (A) Wet SiO_2 solid. (B) Dehydrated SiO_2 solid. (C) Dehydrated TiO_2 solid. The bottom spectrum in A is from the pH 2.1 supernate. The equilibrium pH values of the samples in A and B were (bottom to top): 2.1, 3.2, 3.5, and 4.0. The equilibrium pH values of the samples in C were (bottom to top): 2.1, 3.0, 3.2, and 3.6. All spectra were obtained using pulsed 400 nm excitation and gated detection with 50 us delay. Spectra in C were acquired at LN_2 temperature. All spectra are normalized at the point of maximum intensity.

The spectral data from the UO_2^{2+} / SiO_2 samples dehydrated at 200 °C are shown in Figure 5B. The constancy in the spectral band over the measured pH range is even more striking for these samples. In this respect, the dehydration has the same leveling effect on surface speciation as was observed in the Eu^{3+} samples (vide supra). Here, however,

there is very little difference in the spectral band shape between the wet and the dehydrated samples. Thus, the surface complexes must not change significantly on dehydration in this uranyl system. The measured luminescence lifetimes for the dehydrated samples are also single-exponential denoting a single species, but the lifetime remains constant over the entire pH range here, too. It does, however, appear to increase slightly (258 ± 14 μs from all four samples) relative to the value for the wet samples consistent with the loss of water from the surface environment.

Unfortunately, it was not possible to obtain spectral data for the wet TiO_2 solids containing UO_2^{2+} at either room temperature or ~ 77 K. Even the supernate samples at low pH (those that contained an appreciable amount of unsorbed uranyl) gave only very weak luminescence suggesting that there is a strong quenching interaction between uranyl and dissolved Ti species. It was possible to obtain luminescence data for the dehydrated uranyl / TiO_2 samples. The room temperature data (not shown) are weak, broad, and poorly vibronically structured. However, on cooling these samples to ~ 77 K the spectral data shown in Figure 5C were obtained. There are several important features in this spectral series that distinguish it from the data obtained for the SiO_2 samples. First, the overall spectral band for the TiO_2 samples is shifted to lower energy by ~ 500 cm^{-1} relative to the SiO_2 spectra. This signifies an apparently greater extent of hydrolysis of the surface uranyl species in the TiO_2 samples compared to the SiO_2 samples. One possible mechanism for this is a stronger interaction with the surface titanium hydroxyl oxygens in which there is greater donation of electron density into the uranyl equatorial plane. Alternatively, the bonding interaction on the titanium surface could be of a bidentate nature (i.e., two surface oxygen atoms per uranyl). Either mechanism would be indicative of a stronger surface complex relative to what is observed in the SiO_2 system. The uranyl / TiO_2 spectra also reveal a slight yet monotonic red shift of the spectral bands with increasing pH. The shift amounts to ~ 150 cm^{-1} over the pH range examined and can be observed in both the first and second resolved vibronic bands. This is most likely indicative of a contribution from a second uranyl surface complex that increases in importance with increasing pH. The luminescence lifetime data for these samples support this assertion. The decay curves for all four dehydrated TiO_2 samples require two distinct lifetimes for adequate fits, and the relative contribution to the total intensity of

each lifetime changes with pH. The average values for these two lifetimes are 74 ± 5 μs and 189 ± 6 μs. The observation of a second distinct surface complexation population for uranyl on TiO_2 (but not on SiO_2) probably indicates a difference in the surface itself that gives rise to multiple populations. Again, it is well established in other transition metal oxides (e.g., hematite and ferrihydrite) that both "strong" and "weak" sites exist for sorption of metal cations [30].

Characterization of Surface Complexation on Clay Minerals

The room-temperature time-resolved luminescence spectral data for the Eu^{3+} sorption complexes on SAz-1 and SWy-1 are summarized in Fig. 6. Note that even thought the ICP analytical data for the SAz-1 samples indicate no measurable uptake, there is ample luminescence spectroscopic signal for these samples. The data for the SAz-1 samples are essentially invariant on going from pH 4 to pH 5 over the entire Eu^{3+} concentration range. The relative intensity in the "hypersensitive" transition ($^5D_0$ to $^7F_2$ at ~ 16,200 cm^{-1}) relative to that in the $^5D_0$ to $^7F_1$ transition at ~ 16,860 cm^{-1} indicates a significant reduction in the symmetry of the Eu^{3+} ion relative to, e.g., the fully aquated ion. While this spectroscopic evidence is inconclusive with respect to confirming exchange-site populations in this clay, it is akin to observations made under similar conditions for UO_2^{2+} sorption on SAz-1 [7, 28]. Namely, the environment around the metal ion is not consistent with a fully hydrated coordination sphere. If the metal is in fact in an exchange site, the site is likely unable to accommodate a fully aquated metal ion. It is known that this predominantly Ca^{2+}-exchanged clay has a smaller basal plane spacing than do the Na^+-exchanged materials.

In contrast to the spectral data for Eu^{3+} on SAz-1, the data on SWy-1 show significant variability with both pH and Eu^{3+} loading. At the lowest Eu^{3+} concentrations the spectra at both pH values are similar to those obtained for the SAz-1 samples. This may be indicative of an edge-site population for the metal surface complexes at low loading on this clay. The edge sites are more reactive and form stronger sorption complexes in general than do the exchange sites. Thus, at low loadings, the partitioning of the metal may favor these more reactive sites. At higher metal loadings the relative intensity in the bands at ~ 16,200 and 16,860 cm^{-1} begins to shift reflecting a change in

the symmetry around the metal ion. In fact, at the highest loading at pH 4, the spectrum begins to resemble that found for Eu^{3+} in aqueous solution at pH 4 (c.f., Fig. 3). The pH 5 spectral data at intermediate and high loading levels are intermediate in the relative

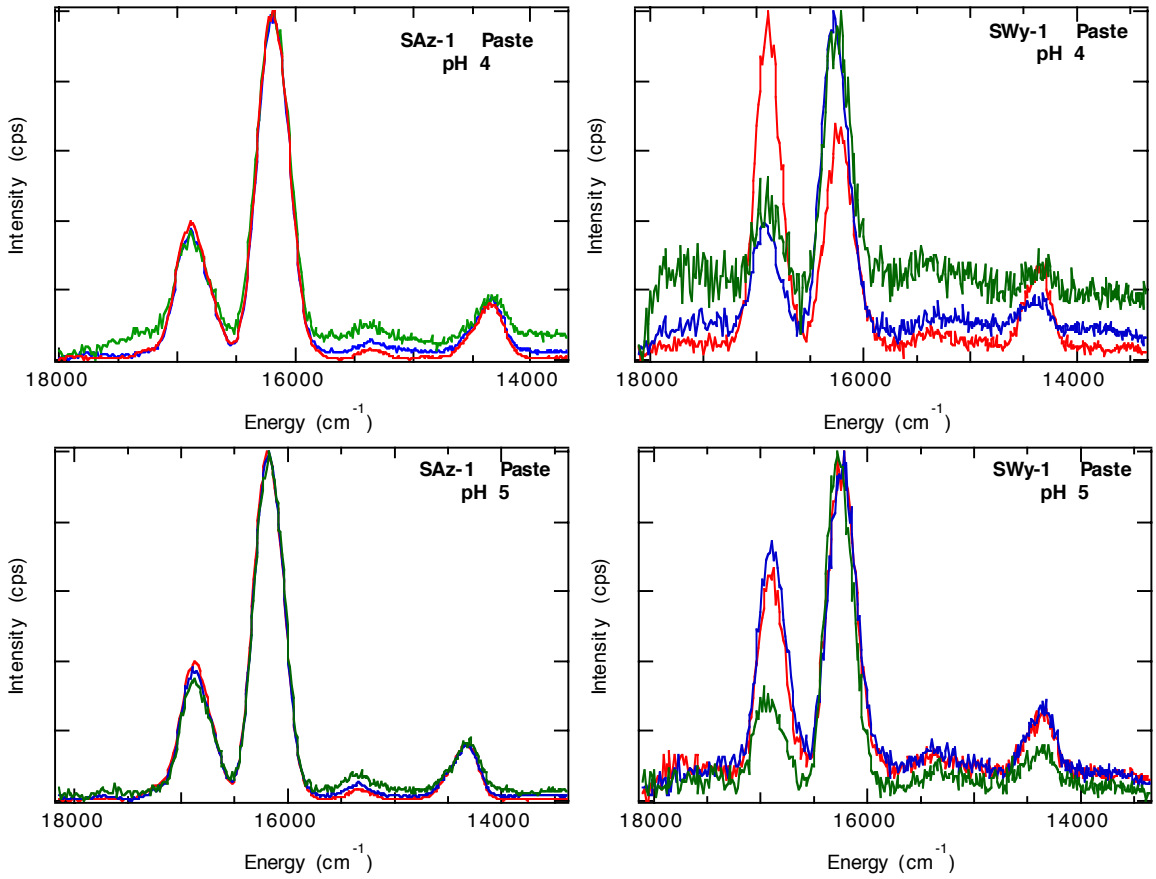

Figure 6. Eu^{3+} luminescence spectra from smectitic clay mineral sample as a function of the initial Eu^{3+} solution concentration: 10 ppm, 50 ppm, and 100 ppm. Spectra were obtained with 393 nm pulsed excitation and gated detection using a 50 microsecond delay. All spectra have been normalized to unit intensity in the most intense spectral band.

intensity of these two main bands. The spectrum for the most highly loaded pH 4 sample on this clay is clearly consistent with a dominant exchange site population. The data for the pH 5 samples may reflect a mixture of edge and exchange site populations (hence the intermediate intensity data) or a difference in the metal speciation within the exchange sites. Notably, on drying at room temperature and ambient humidity, the spectral data (not shown) for all samples converge to the same general characteristics and look very

similar to those seen for the SAz-1/pH 4 samples. It is known that drying leads to expulsion of interlayer water and a collapse of the spacing between basal planes. Thus, this transition for the SWy-1 clays in good evidence of a highly hydrated Eu^{3+} exchange population that is transformed to a less well hydrated population on drying.

The interpretations of the luminescence lifetime data obtained for these samples are generally consistent with the spectral domain data interpretations. Nearly all samples exhibit multiple exponential decay behavior suggesting multiple surface complex populations. However, one lifetime dominates in essentially all samples. Using this dominant lifetime, the number of coordinated water molecules was determined by the formula provided above. These results are summarized in Table 1. The hydration

Table 1. Hydration of Surface Eu3+ on Smectites from Luminescence Lifetime Data

Sample		$[Eu^{3+}]$init (ppm)		
		10	50	100
		n_{H2O}		
SAz-1 / pH 4	Wet	2.1	2.5	3.5
	Dry	1.1	0.9	1.1
SAz-1 / pH 5	Wet	4.4	3.6	3.2
	Dry	1.1	1.2	1.2
SWy-1 / pH 4	Wet	3.1	2.5	6.8
	Dry	3.4	5.9	5.1
SWy-1 / pH 5	Wet	2.8	3.9	2.3
	Dry	3.9	4.4	3.8
R-9 / pH 4	Dry	3.2	3.1	4.2
LK-1 / pH 4	Dry	4.2	2.8	3.3

number for the SWy-1 sample prepared from the 100 ppm Eu^{3+} solution does approach the value for the fully aquated ($n_{H2O} = 9$) cation. There is surprisingly little impact on the hydration numbers for the wet vs. dry samples with the SWy-1 clay. The hydration

numbers for Eu^{3+} in the soil clay isolate samples (R-9 and LK-1) are similar to those for the SWy-1 clay.

Electrochemical Studies in Homogeneous Solution

Electron transfer between a dissolved redox-active species and an electrode surface is intrinsically a kinetically controlled process. When the electron transfer step per se is facile, there are typically no manifestations of the electron-transfer kinetics in the electrochemical response (e.g., from cyclic voltammograms) and the process obeys diffuse controlled kinetics. In this case, the voltammetric data reflect the thermodynamic properties of the system. This diffusion-controlled regime is an important one because it does provide information about the energetics of the electron transfer (i.e., the ease with which a species can be reduced or oxidized). However, it is frequently true, particularly for f-element complexes, that there is also a kinetic barrier to electron transfer. Under such circumstances the voltammetry will manifest a response indicative of both electron-transfer and diffusion-controlled kinetics, and the data can be analyzed to extract the kinetics of the intrinsic electron-transfer step. The sluggish electron-transfer kinetics are nominally associated with a reorganizational barrier associated with the electron-transfer step.

The target f-element analytes used in the work described here, Eu^{3+} and UO_2^{2+}, both undergo one-electron reduction processes, and for both it is common to find manifestations of sluggish electron-transfer kinetics in the voltammetric response. Surprisingly, however, little attention has been devoted to cataloging and understanding this behavior. Thus, the starting point for the efforts in this project was to establish a baseline for electron-transfer kinetic behavior in solutions of dissolved metals and metal complexes before tackling the redox kinetics and energetics governing the same metals associated with metal oxide colloids. A survey of the voltammetric behavior of the $UO_2^{2+/1+}$ couple for six different metal coordination environments is shown in Fig. 7.

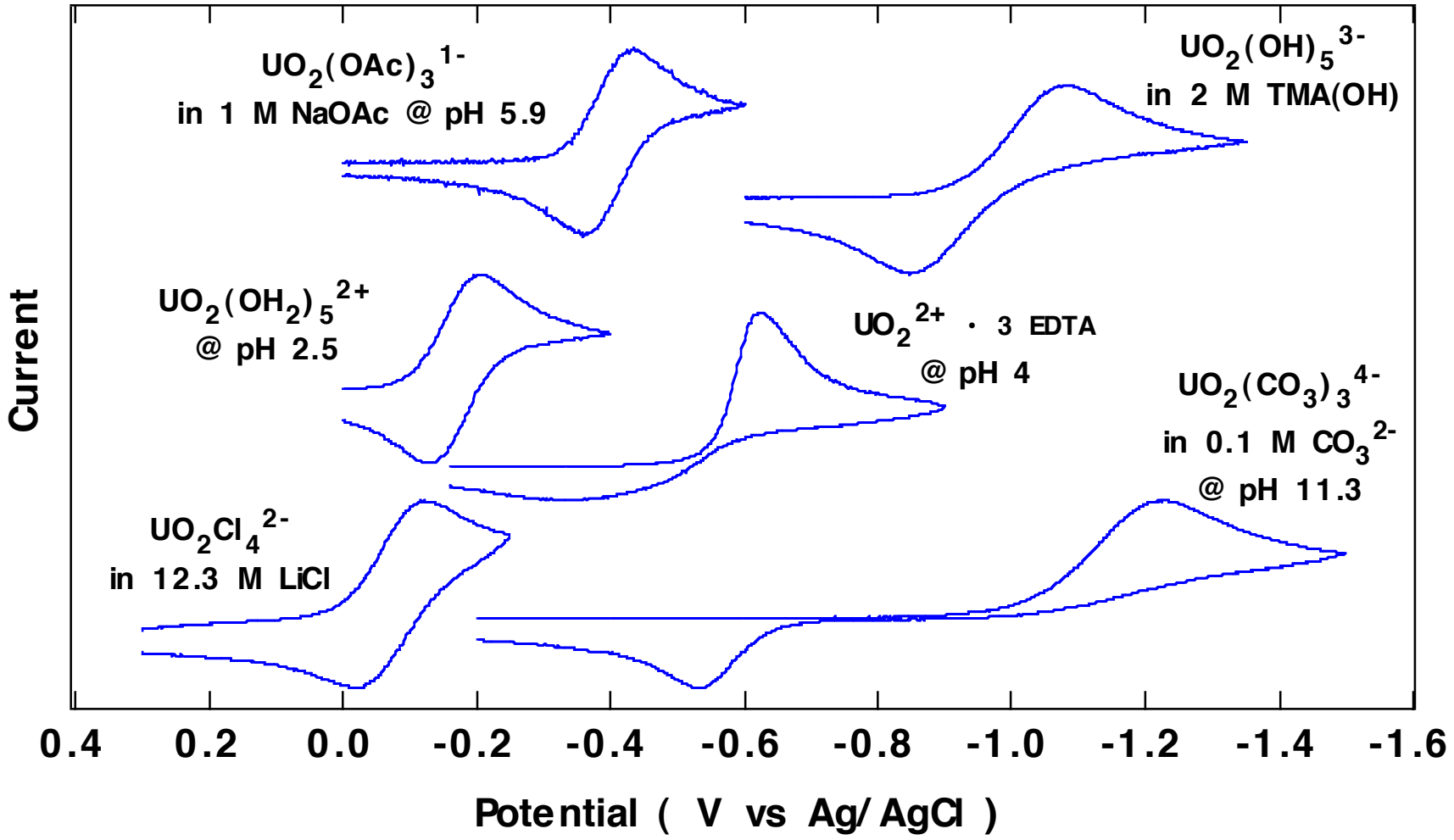

Figure 7. Cyclic voltammograms for the UO22+ / UO2+ redox couple in aqueous solutions as indicated. The scan rate for each voltammogram was 100 mV/s. All systems except the 12.3 M LiCl were studied at a hanging Hg drop electrode. A Pt microdisk was used in 12.3 M LiCl.

Note the incredibly wide variation in both the half-wave potential for the uranyl couple and the difference in the rates of electron transfer. Cyclic voltammograms such as those shown in Fig. 7 have been analyzed as a function of the potential scan rate to extract both the thermodynamic and kinetic parameters characterizing the redox process. The analysis is based on digital simulations using a method described by us previously [31]. A typical data fitting result is shown in Figure 8. The metrical data from these analyses are provided in Table 2.

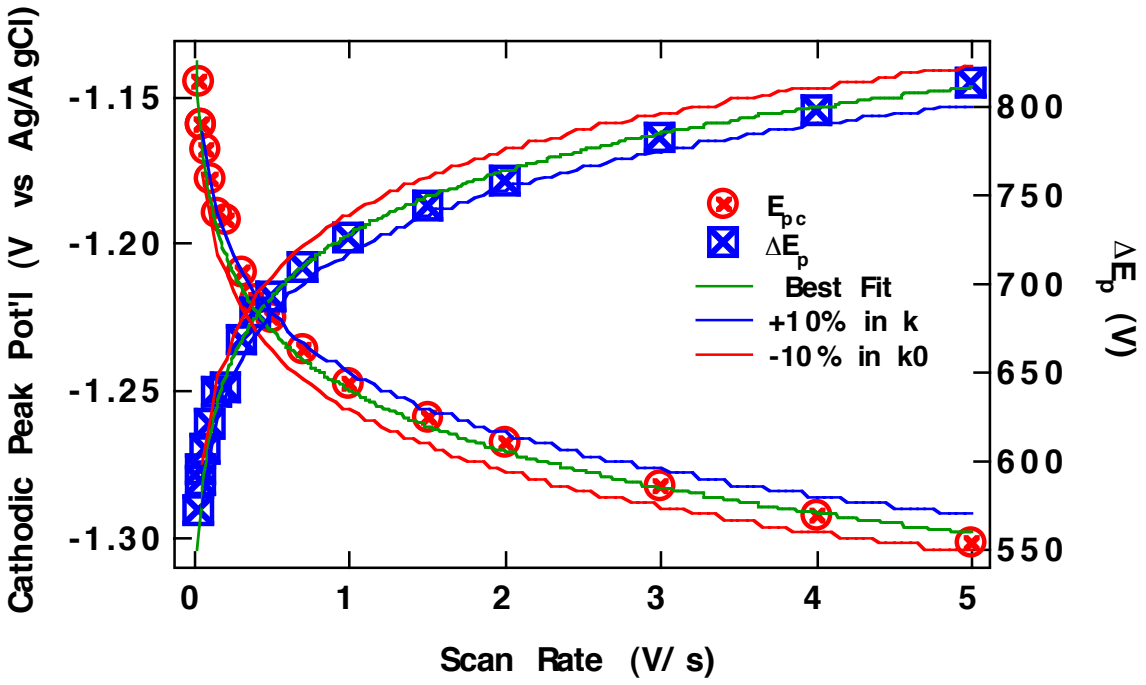

Figure 8. Best fits(solid green lines) to the cyclic voltammetric data (E_{pc} and $\Delta E_p = E_{pc} - E_{pa}$) vs. scan rate for the redox couple $[UO_2(CO_3)_3]^{4-} + e^- = [UO_2(CO_3)_3]^{5-}$ in 0.1 M CO_3^{2-} solution at pH 11.3 using digital simulations of the voltammetric response. The sensitivity of this method (and thus the accuracy of the derived kinetic parameters) is indicated by the ± 10% variability in the quality of the fits(solid blue and red lines).

The variability in the half-wave potentials for the uranyl couples are clearly related to the basicity of the coordinating ligands. More strongly electron donating equatorial ligands such as hydroxide and carbonate shift the reduction potential to more negative values relative to the aquated cation by nearly 1 V. The variability in the electron transfer kinetic parameters is far less straightforward to explain. As noted above, sluggish kinetics are typically associated with large reorganizational barriers

accompanying the process, e.g., significant bonding changes associated with the addition or removal of the electron. This effect should be much more subtle in the case of f-based redox orbitals because these do not engage significantly in bonding. We are continuing to explore this effect through examination of bond-length changes for AnO_2^{2+} vs. AnO_2^{+} ions in identical coordination environments. Detailed data for this comparison are sparse, but are becoming more available as progress is made in x-ray absorption spectroscopic studies [32].

Table 2. Homogeneous Redox Kinetic and Thermodynamic Data for Analyte Complexes

System	k^0 (cm/s)	α	$E_{1/2}$ (V vs Ag/AgCl)
$[Eu(OH_2)_9]^{3+/2+}$	1.25×10^{-4}	> 0.5	-0.60
$[UO_2(C_2H_3O_2)_3]^{1-/2-}$	≥ 0.1[a]	~0.5	-0.400
$[UO_2Cl_4]^{2-/3-}$	9.2×10^{-3}	0.30	-0.065
$[UO_2(OH_2)_5]^{2+/1+}$	9.0×10^{-3}	0.50	-0.169
$[UO_2(OH)_5]^{3-/4-}$	2.82×10^{-3}	0.46	-0.927
$[UO_2(CO_3)_3]^{4-/5-}$	2.6×10^{-5}	0.41	-0.820

[a] Too fast to measure by cyclic voltammetry.

Heterogeneous Electrochemical Studies

The thermodynamic and kinetic aspects of electron-transfer processes to the analytes (Eu^{3+} and UO_2^{2+}) associated with the metal-oxide substrates (SiO_2 and TiO_2) were investigated using the same samples for which sorption reactions and surface spectroscopic characterizations had previously been conducted. To derive information directly pertinent to the properties of the surface-bound species, it was necessary to isolate the solid oxides following the sorption reactions (i.e., to remove supernate containing unsorbed analyte species) and resuspend this material in fresh solution prior to voltammetric interrogation. In addition, voltammetric data were collected directly on the sorption reaction supernates to provide a comparison with data obtained for the substrate-bound materials. The sorption process is, of course, an equilibrium phenomenon. Thus, the process of resuspending the isolated oxide substrates in fresh solution certainly leads

to some desorption of the analyte species into bulk solution. Furthermore, the sorption process is also a dynamic one. Thus, rapid exchange between bulk solution and the surface is probable. The consequence of these considerations is that the voltammetric data for the oxide suspensions likely contains some contribution from dissolved analyte species as well. For this reason, following the voltammetric studies of the oxide suspensions, the solid phase was again separated by centrifugation and the supernate was re-examined voltammetrically to assess the amount of analyte that desorbed. The voltammetric signal obtained from these supernates was much less (typically less than 5%) than that observed in the suspension samples. Voltammetric investigations of the suspensions were also conducted in unstirred vs. stirred solutions. This approach was intended to provide an assessment of diffusive vs. convective contributions to the total current. Except for the anticipated change in the shape of the voltammetric response, there was little difference in the stirred vs. unstirred experiments (i.e., the potentials at which redox activity was noted remained nearly identical).

One of the more notable features in the voltammetric behavior of the Eu^{3+}-bearing SiO_2 and TiO_2 suspensions was a post-peak "sorption" wave in the single-scan voltammograms. This behavior is illustrated for the TiO_2 suspensions in Fig. 9. The "sorption" wave occurs at slightly more negative potentials than the main voltammetric reduction wave, and it is much more pronounced for the TiO_2 suspensions than the SiO_2 suspension. This behavior is likely the result of a direct interaction between the suspended oxide colloid and the Hg electrode surface. This behavior is commonly observed when dissolved analytes interact directly with the surface of the electrode. However, it has never been observed in homogeneous solutions of Eu^{3+}, leading to the conclusion that it is the colloid/electrode interaction that gives rise to the phenomenon in this case. Notably, the "sorption" wave is lost in all cases on the second and all subsequent voltammetric scans and can only be restored by allowing the system to reequilibrate under open-circuit potential conditions.

Except for this interesting colloid/electrode interaction behavior, there are few other significant differences in the voltammetry of Eu^{3+} on the colloid surface vs. that observed in the neat (homogeneous) sorption-reaction supernate. This is illustrated in the voltammograms for Eu^{3+} on SiO_2 shown in Fig. 10, and the same behavior is observed on

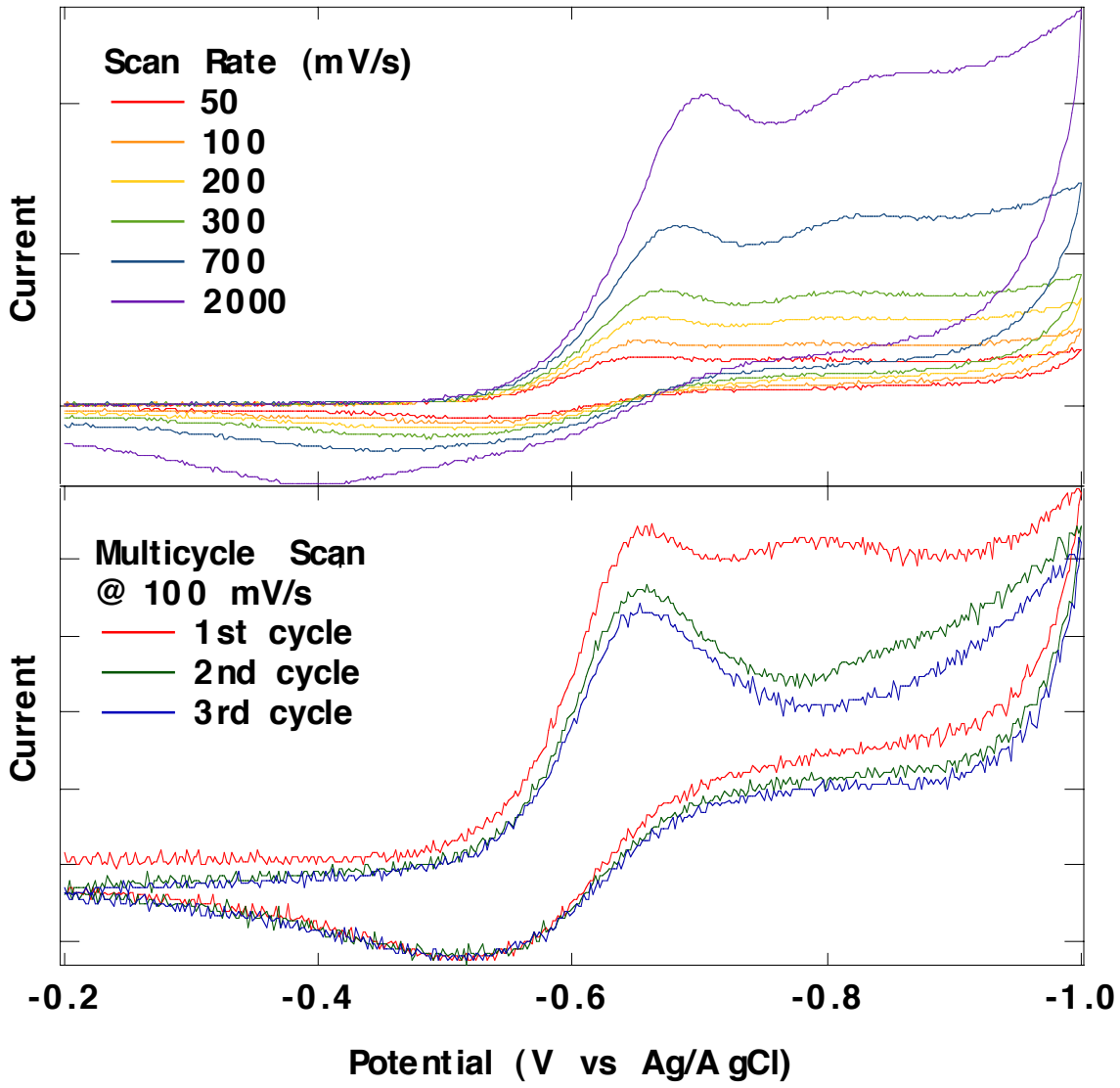

Figure 9. Cyclic voltammetric data for $Eu^{3+} + e^{-} = Eu^{2+}$ *in an aqueous suspension of* TiO_2 *obtained at an Hg drop electrode.*

TiO_2. Thus, there appear to be no significant perturbations in either the redox thermodynamics or the electron-transfer kinetics for Eu^{3+} on the surface vs. in bulk solution. There is also little if any pH effect on these properties. These observations quite consistent with the spectroscopic data discussed above for the Eu^{3+} surface speciation on the oxide substrates. Even at the highest sorption reaction pH values the surface species retains a hydrated coordination environment. Thus, the redox orbitals are not significantly perturbed via extensive interaction with surface hyroxyl groups and no

substantial inner-sphere structural reorganization is required in concert with the redox process.

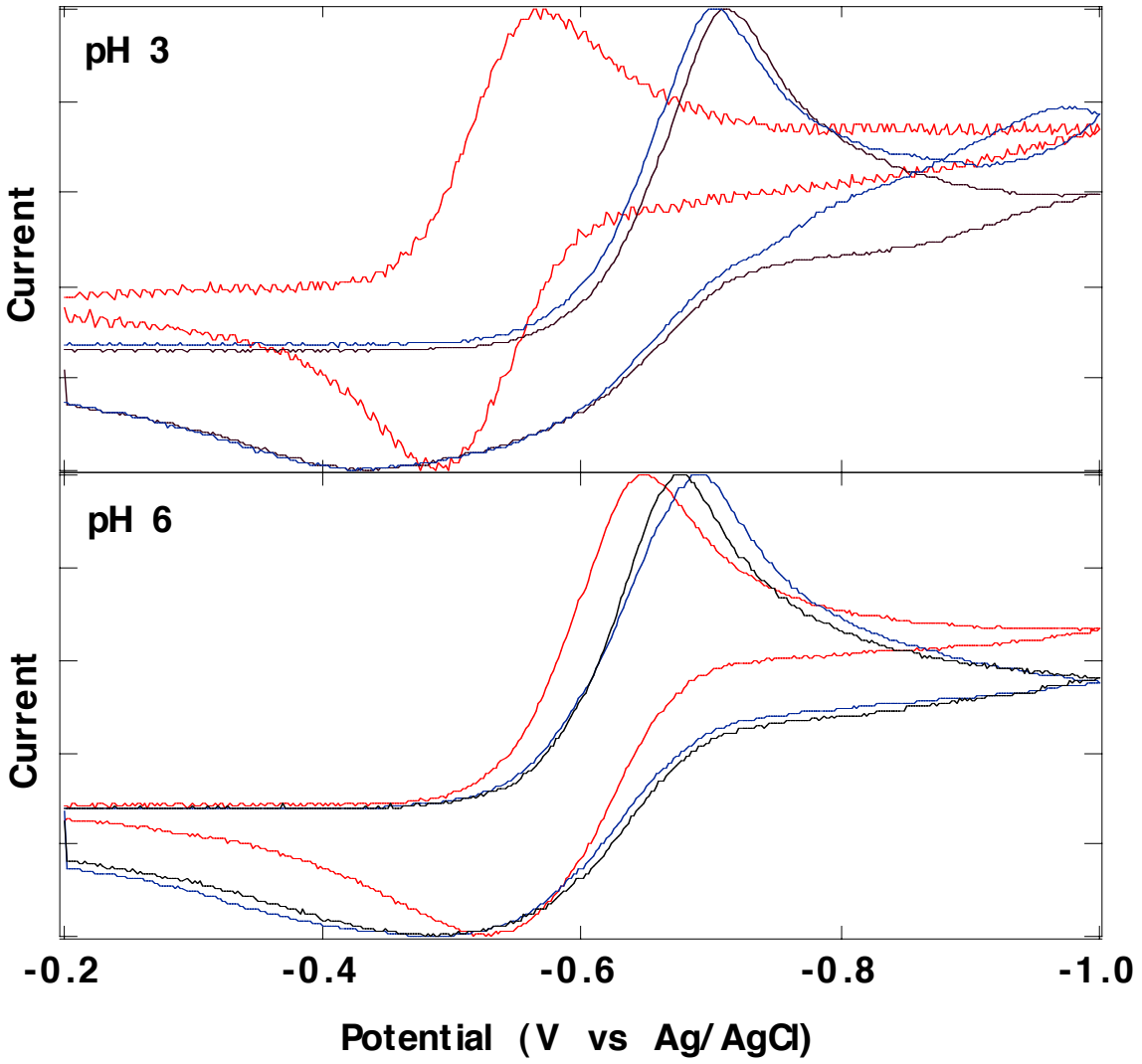

Figure 10. Cyclic voltammetric data for aqueous suspensions of Eu^{3+} sorbed on SiO_2. Blue curve is for the suspension isolated from the sorption reaction mixture. Red curve is for the suspension following dehydration at ~ 200 °C and resuspension in aqueous electrolyte. Black curve is for the supernate from the initial sorption reaction. All voltammograms have been normalized to the same current full-scale to facilitate comparison. The scan rate is 50 mV/s.

In contrast to the behavior for the fully hydrated suspension, the voltammetric behavior for the oxide suspension that first underwent dyhydration at ~ 200 °C (see

Experimental) prior to resuspension in aqueous solution for the voltammetric studies is markedly perturbed. These results are also illustrated in Fig. 10. For these "baked"suspension the voltammetry indicates a perturbation in both the redox thermodynamic characteristics of the surface species and the electron-transfer kinetics. Specifically, note that the redox potential for the baked species has shifted to more positive values relative to the oxide samples that did not undergo dehydration (and the neat reaction supernate). The potential shift between the "baked" and fully hydrated samples was found to be pH dependent, ranging from ~ 150 mV at pH 3 to ~ 30 mV at pH 6. The perturbation in the electron-transfer kinetics is equally pronounced, and it too is pH dependent. Note that at pH 3 (Fig. 10) the voltammogram for the "baked" suspension is nearly fully reversible (symmetric signal with peak-to-peak separation of ~ 60 mV) indicating that the electron-transfer step is quite fast. At pH 6 the voltammogram again adopts the quasi-reversible character of slow electron-transfer, but to a much lesser extent than that of the fully hydrated species or the neat reaction supernate species.

Thus, the process of dehydration (as would be expected for the calcined plutonium oxides) leads to surface Eu^{3+} species on these oxide substrates that are easier to reduce in both energetic and kinetic terms. Here, too, these results are consistent with the spectroscopic characterization data that confirm that the Eu^{3+} in the dehydrated suspensions undergoes significant loss of coordinated water and transforms into a less symmetrical coordination environment attributed to a stronger surface interaction, and this change is not reversed on resuspension in the aqueous electrolyte solution. Apparently both these structural factors give rise to more favorable redox behavior for the surface Eu^{3+} species.

The voltammetric behavior of UO_2^{2+} on the oxide suspensions is much less well-behaved and less reproducible in general than that for the Eu^{3+} suspensions. In particular, the behavior of uranyl on TiO_2 suspenions is totally irreproducible and led to no significant conclusions. Further, no data have been collected to date for the dehydrated uranyl /oxide suspensions because the project concluded before these data could be collected. However, reproducible and quite interesting data were obtained for the uranyl / SiO_2 system as illustrated in Figure 11.

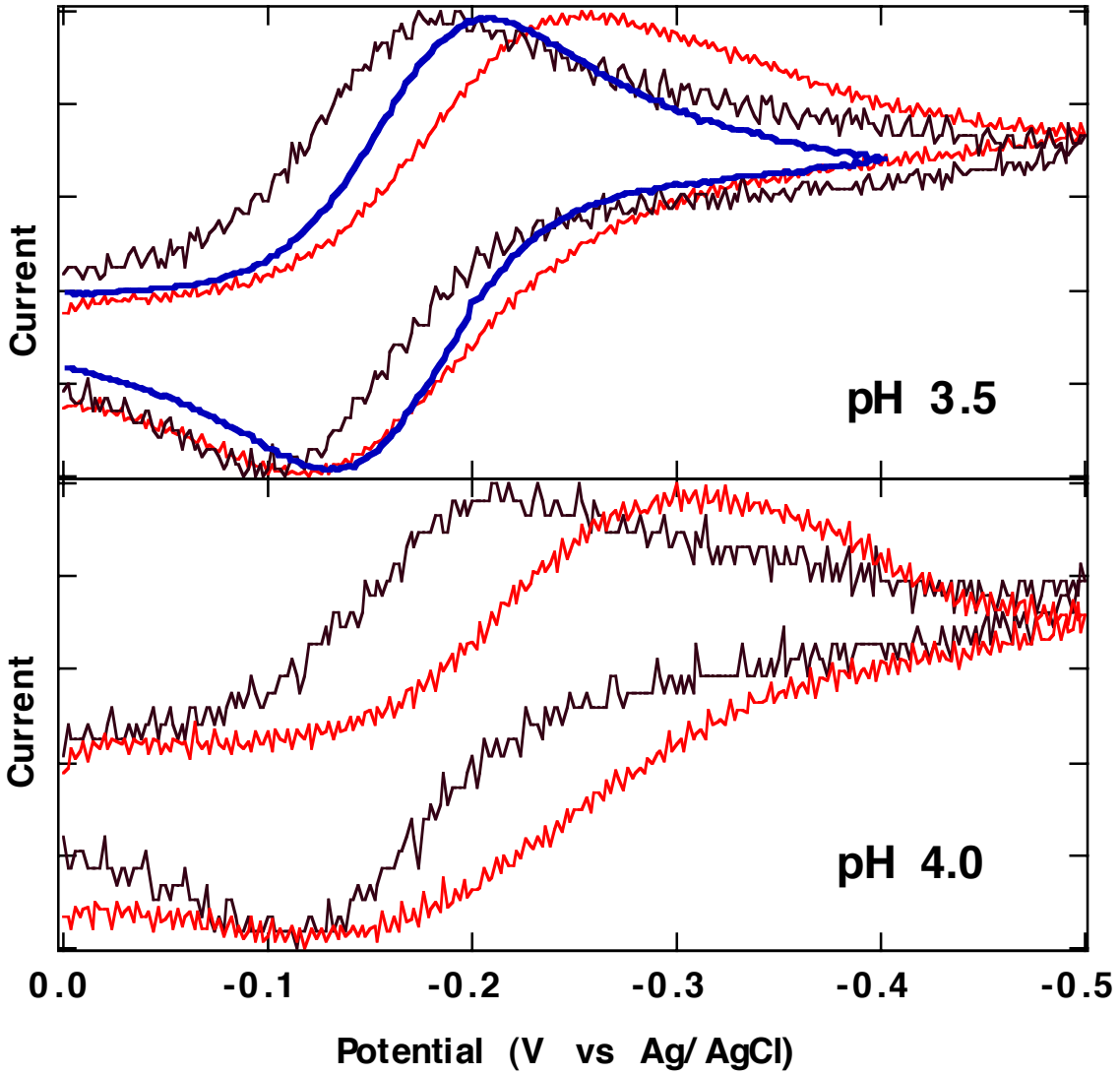

Figure 11. Cyclic voltammetric data for aqueous suspensions of UO_2^{2+} sorbed on SiO_2. Blue curve is for neat aqueous solution of uranyl (~10 mM) at pH 2.5. Red curves are for the oxide suspensions at the pH indicated. Black curves are for the sorption reaction supernates at the pH indicated. All voltammograms have been normalized to the same current full-scale to facilitate comparison. The scan rate is 50 mV/s.

Unlike the behavior observed for the Eu^{3+}/oxide systems, for the UO_2^{2+} / SiO_2 system there is a big difference in the voltammetric behavior for the fully hydrated, surface-bound species vs. that seen in the homogeneous sorption reaction supernate. This difference is manifest in both the redox thermodynamics and the electron-transfer kinetics. Specifically, note that the redox potential for the surface-bound species shifts to

more negative values by ~ 50 mV relative to that for the supernate, and the peak-to-peak potential separation that reflects the ease of electron-transfer kinetics increases substantially for the surface-bound species relative to the homogeneous species from the reaction. There is also a modest pH dependence associated with these effects, but much less so than observed for the "baked" Eu^{3+} suspensions.

These results for the uranyl / oxide system relative to the Eu^{3+} / oxide system (fully hydrated in both cases) are again consistent with the differences in the nature of the surface complexes as revealed by the spectroscopic characterization. In particular, there is ample evidence that the uranyl species interact with the oxide surfaces much more strongly than do the Eu^{3+} species. This stronger metal-surface oxygen interaction is tantamount to oxohydroxide coordination to the metal in bulk solution (e.g., from a hydroxide ligand) and gives rise to a similar shift to more negative values in the redox potential (c.f., Fig. 7), although for the suspension the effect is much less dramatic (~ 50 mV vs. ~ 1 V for the true hydroxide complex). Also in a manner similar to the homogeneous hydroxide complex, the electron-transfer kinetics become more sluggish for UO_2^{2+} on the SiO_2 surface.

Advances in MEO/R Processing

One aspect of this project is to determine the dissolution kinetics of plutonium species entrained on the surface of solid materials. An example of a solid material that is ubiquitous throughout the nuclear complex is spent ion exchange resin that is used in plutonium recovery operations. These resin materials gradually lose their efficacy, presumably due to radiation damage from the absorbed actinide elements. This radiation damage can significantly alter the structure of the resin through free radical bond cleavage and recombination. In some cases the elements absorbed on the resin may become encapsulated and no longer available for elution. The mediated electrochemical oxidation process is capable of destroying the resin's organic matrix and liberating the encapsulated metallic ions. Part of this work was devoted to an investigation of the kinetics of the destruction of an industry standard cation exchange resin using three electron transfer mediators, cobalt(III), silver(II) and cerium(IV), in both nitric and

sulfuric acid media. The goal of this study was to determine the conditions for optimum reaction efficiency.

The complete oxidation of a sulfonated styrene unit of a standard cation exchange resin proceeds according to reaction 1:

$$C_8H_8SO_3H + 17\ H_2O \rightarrow 8\ CO_2 + SO_4^{2-} + 43\ H^+ + 41\ e^- \qquad \text{(Eqn.1)}$$

Each of the resin destruction experiments was run at a current of 1 ampere for 3 hours, a quantity of electricity sufficient to destroy approximately 0.51 grams of resin at 100 percent current efficiency. The average loss in weight of the resin was approximately 2-3 percent, verifying the chemically inert nature of this material even at elevated temperatures in strongly oxidizing nitric acid solution.

The oxidizing power of the three mediators chosen increases in the order Ce(IV)<Ag(II)<Co(III). At room temperature the disappearance of resin from the solution follows this same trend. With cerium(IV), the weakest of the oxidants, there is essentially no reaction. Using silver(II) or cobalt(III) as mediator at 0.1 M concentration, the reaction proceeds smoothly, with the amount of resin destroyed exceeding the theoretical amount possible based solely on the number of coulombs of electricity passed. Two possible explanations exist for this behavior. First, the resin may not react completely to produce carbon dioxide, but instead form a water soluble intermediate. However, when a deficiency of resin is used instead of an excess, analysis of the resulting solution typically gives results in the order of 100 ppm total dissolved organic carbon. Thus the reaction will proceed to completion. A second possible explanation is that while the resin itself is resistant to chemical attack by the strongly oxidizing nitric acid media, the intermediate products generated are not.

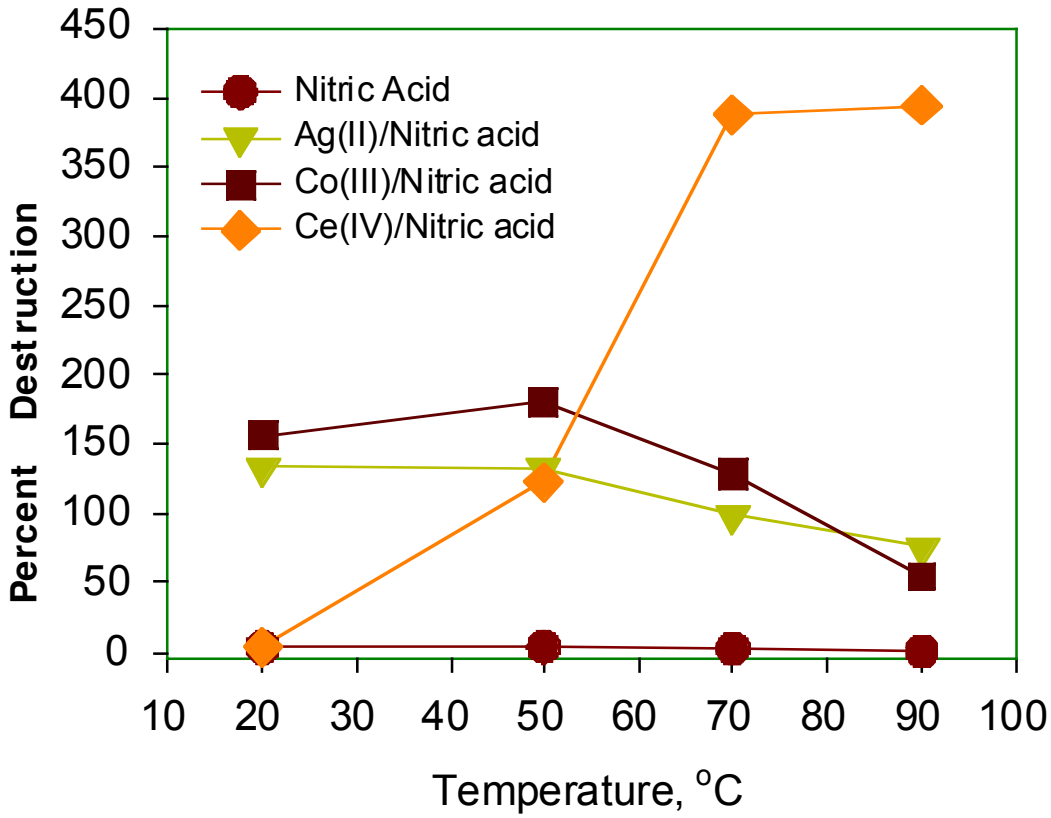

When the temperature is raised to 50 ° C, the resin destruction efficiency using silver(II) and cobalt(III) as mediators is slightly greater than at room temperature, but the solution never develops the characteristic colors associated with the ions in their higher oxidation states. Two reactions are occurring simultaneously, reaction of the mediator with the resin and reaction of the mediator with solvent, as given in equation 2.

$$2\ H_2O + 4\ Co^{3+} \rightarrow O_2 + 4\ Co^{2+} + 4\ H^+ \qquad \text{(Eqn.2)}$$

The former reaction is expected to proceed at a faster rate at elevated temperatures, but the latter reaction, which also proceeds at a faster rate, lowers the effective mediator concentration. Thus raising the temperature appears to have little effect on the resin destruction rate. If the temperature is raised still further, to 70 °C and 90 ° C, the resin

destruction efficiencies with silver and cobalt gradually decrease. The deleterious solvent/mediator reaction rate begins to exceed that of the mediator/resin reaction.

The efficiency of resin destruction using cerium(IV) as mediator increases dramatically as the temperature is raised. From essentially an immeasurably low reaction at room temperature it increases to greater than 100% destruction efficiency at 50 °C, comparable to the efficiency observed with silver(II). At 70 °C, the efficiency approaches a phenomenal 400%, far exceeding either cobalt(III) or silver(II). At 90 °C, the efficiency ceases to increase signaling the onset of the solvent reaction with cerium(IV).

Trends observed in sulfuric acid media mimic those seen in nitric acid but in less dramatic fashion. With cobalt(III) as mediator there is a slight gradual decrease in destruction efficiency as the temperature is raised. With cerium(IV) there is essentially no reaction at room temperature but a steady increase in reaction efficiency with increasing temperature. Destruction efficiency in excess of 100 percent of theoretical is not observed with either mediator. This observation lends further validity to the assumption that nitric acid contributes to the oxidation process while the non-oxidizing sulfuric acid does not.

Experiments to measure the reaction kinetics and stoichiometry were carried out using cerium(IV) in nitric acid. Cerium(IV) was chosen due to its stability in aqueous solution at moderate temperatures while both cobalt(III) and silver(II) are not. In these experiments the cerium(IV) concentration was monitored spectrophotometrically with time following addition of resin. When a deficiency of resin was used the change in absorbance was used to calculate the quantity of cerium(IV) necessary to completely oxidize a given weight of resin. The average value obtained for three runs at 52 °C was 18.5 equivalents of cerium(IV) per equivalent of resin. The value is considerably lower than the theoretical value of 41 equivalents. Yet analysis for total organic carbon demonstrated essentially no soluble organic material remaining in solution.

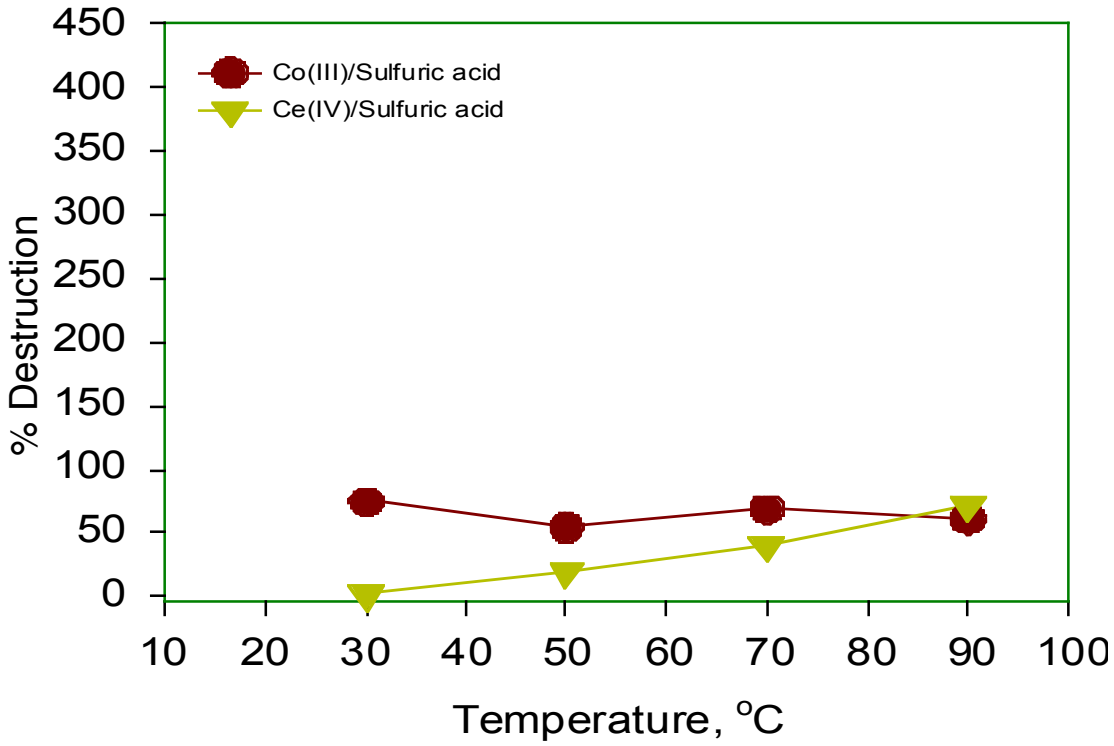

Methods Development

A very important aspect of the proposed work is highly accurate and precise determinations of redox potentials (~ 1-2 mV precision) to properly measure stability constants for surface complexes and metal complexes. This presents serious challenges with existing commercially-available reference electrodes. In particular, reference electrode potentials drift due to changes in liquid junction as a result of differing ion migration rates in strongly acidic media. Furthermore, precipitation of salts occurs at the interface between the reference electrode and the test solution as a consequence of exceeding salt solubility in strongly ionic media. Finally, the outer electrode filling solution must contain an ion that will not form a complex with metals such as plutonium since it is in contact with test solution. To circumvent these problems an new reference electrode was designed and tested. The new design replaces the conventional fill solutions (KCl and KNO_3) with perchlorate solutions.

Another important capability for this project is the determination of voltammetric data for Pu under dilute solution conditions. Even in relatively acidic solutions (e.g., pH 0 to 1) plutonium is only sparingly soluble. Thus, highly sensitive voltammetric methods

must be employed. To this end, calibration curves for Pu in 0.1 and 0.092 M acid solution using square wave voltammetry on a platinum electrode have been constructed for use in the analyses of sorption samples. The results look very promising with a concentration range from 20 to 200 ppm and a lower detection limit of ~10 ppm.

Relevance, Impact, and Technology Transfer:

Q. How does this new scientific knowledge focus on critical DOE environmental management problems?

A. This question is addressed in the Research Objectives section on pp. xx

Q. How will the new scientific knowledge that is generated by this project improve technologies and cleanup approaches to significantly reduce future costs, schedules, and risks and meet DOE compliance requirements?

A. This question is addressed in the Research Objectives section on pp. xx

Q. To what extent does the new scientific knowledge bridge the gap between broad fundamental research that has wide-ranging applications and the timeliness to meet needs-driven applied technology development?

A. While the research conducted under the work-scope of this proposal is fundamental in nature, it has direct and immediate applicability the areas of understanding / predicting redox behavior of important actinide species entrained in solid matrices.

Q. What is the project's impact on individuals, laboratories, departments, and institutions? Will results be used? If so, how will they be used, by whom, and when?

A. It is unclear to what extent the DOE in general and the Nuclear Materials Focus Area in particular are willing to consider reprocessing of lean processing residues for volume reduction and/or stabilization. If residue processing does become a viable consideration, the results generated within this project will have immediate practical application.

Q. Are larger scale trials warranted? What difference has the project made? Now that the project is complete, what new capacity, equipment, or expertise has been developed?

A. Large-scale trials of the research conducted under this project are not currently warranted. However, small-scale trials with actual Pu-bearing residues should be undertaken.

Q. How have the scientific capabilities of collaborating scientists been improved?

A. Not applicable for this project.

Q. How has this research advanced our understanding in the area?

A. The impact here has been two-fold. First, the results have led to a specific new understanding of the role of surface interactions of metal ions with surfaces in modifying redox properties. Second, the project has developed and demonstrated a new experimental protocol for assessing these effects that can be used for assessing redox properties in other important substrates such as ceramics and glasses under consideration as waste forms.

Q. What additional scientific or other hurdles must be overcome before the results of this project can be successfully applied to DOE Environmental Management problems?

A. No significant hurdles remain in using the results of this study in real-world applications.

Q. Have any other government agencies or private enterprises expressed interest in the project? Please provide contact information.

A. There have been numerous (> 10) contacts from individuals seeking information on the surface spectroscopic characterization methods used in this and other DOE investigations, but no specific contacts regarding MEO/R applications for residue processing.

Project Productivity:

The work-scope set forth in the original project proposal was downsized to reflect the actual budget allocation ($ 250 k/yr for 3 years) vs. the requested budget ($ 400 k/yr for 3 yrs). The tasks that were sacrificed included scale-up studies using actual Pu residues and some of the redox studies using mediators to alter the redox properties. Within the context of this revised work-scope nearly all project goals were accomplished. Several experiments were not completed (e.g., the redox studies of the metal-bearing clay minerals), but efforts to finish this work outside the scope of the current project are underway.

Personnel Supported:

The following is a list of personnel who derived support from this grant and/or contributed to the research effort during the three-year grant cycle along with their current position and affiliation:

David E. Morris (Project PI)	Technical Staff Member/ Chemistry Division	Los Alamos National Laboratory
Carol J. Burns	Deputy Division Leader / Chemistry Division	Los Alamos National Laboratory
Wayne H. Smith	Technical Staff Member /Materials Science and Technology Division	Los Alamos National Laboratory
Deborah S. Ehler	Technician - 7 / Chemistry Division	Los Alamos National Laboratory
C. Thomas Buscher	Technician - 7 / Chemistry Division	Los Alamos National Laboratory
David L. Blanchard, Jr.	Senior Research Scientist II / Separations and Radiochemistry	Pacific Northwest National Laboratory
Tammy A. Diaz	Graduate Student	University of Nevada, Las Vegas
Kristin Little	Undergraduate Student	Furman University

Ms. Diaz, a rising senior environmental geology major at New Mexico Highlands University when she worked as a summer research intern on this project in FY 1999, was awarded a U. S. Department of Energy 1999-2000 DOE Environmental Management Scholarship Program Hispanic Scholarship Fund grant.

Ms. Little, a rising junior chemistry major at Furman University when she worked as a summer research intern on this project in FY 2000, is using her work as the basis for her senior research thesis in fulfillment of departmental degree requirements.

Publications:

Peer-Reviewed Manuscripts

In Print

1. Eu^{3+} and UO_2^{2+} Surfaces Complexes on SiO_2 and TiO_2. T. A. Diaz, D. S. Ehler, C. J. Burns, and D. E. Morris. *ACS Symposium Series* **2001**, 778, 83-97.

In Preparation

1. Variation in the Electron-Transfer Kinetic Properties of the UO22+/1+ Redox Couple as a Function of Coordination Environment. D. E. Morris, manuscript in preparation.
2. Probing the Exchange Sites in Smectites by Europium(III) Luminescence. K. Little and D. E. Morris, manuscript in preparation.

Reports

1. Aqueous electrochemical mechanisms in actinide residue processing. Morris, D. E. ; Blanchard, D. L., Jr.; Burns, C. J.; Smith, Wayne H. June 1, 1999 LA-UR-99-2911

2. Aqueous electrochemical mechanisms in actinide residue processing. Morris, D. E. 1998 LA-UR-98-2318

Interactions:

Participation & Presentation at Meetings and Workshops

1. "Aqueous Electrochemical Mechanisms in Actinide Residue Processing." DOE Environmental Management Science Program Scientific Workshop, Chicago, IL, July 27-30, 1998.
2. "Trends in Actinyl Electrochemistry: Voltammetry and Theory." 217th National Meeting of the American Chemical Society, Anaheim, CA , April 21-25, 1999.
3. "Aqueous Electrochemical Mechanisms in Mediated Dissolution of Actinide Residues." 218th National Meeting of the American Chemical Society, New Orleans, LA, August 22-26, 1999.

4. “Aqueous Electrochemical Mechanisms in Actinide Residue Processing.” DOE Environmental Management Science Program National Workshop, Atlanta, GA, April 24-27, 2000.

5. “Probing Exchange Sites in Smectitic Clays Using Europium(III) Luminescence.” National Conference for Undergraduate Research, University of Kentucky, Lexington, Kentucky, March 15th, 2001.

Transitions:

a. Describe cases where knowledge resulting from your effort is used, or will be used, in a technology, technique, or process improvement application. Transitions can be to entities in DOE, other federal agencies, or industry.

It became clear during the second year of this project from interactions with participants in the Nuclear Materials Focus Area that the likelihood of any near-term reprocessing of lean Pu processing wastes by any technology was minimal. The emphasis of this focus area has shifted and continues to be on stabilization of oxide in 3013 storage containers. This waste matrix is down-stream of the residue materials under consideration in the project described here. Our emphasis shifted somewhat in response to this change of focus to develop a more fundamental yet robust approach to understanding redox properties for actinides entrained in essentially any matrix. Thus, our work has conceivable bearing on evaluation of waste matrix stability for ceramics and glasses as well as processing residues.

b. Briefly list the enabling research, the laboratory or company, and an individual in that organization who made use of your research.

Not Applicable to this Project.

Patents: None.

Future Work:

Several experiments were not completed (e.g., the redox studies of the metal-bearing clay minerals), but efforts to finish this work outside the scope of the current project are underway. Some of the experiments proposed in the initial project proposal (i.e., prior to rescoping in the face of a diminished budget) should still be conducted to enhance to overall impact of this work. Specifically, some experiments using actual Pu processing residues should be undertaken and experiments with homogeneous chelator/redox mediators should be done.

Literature Cited:

1. Defense Nuclear Facilities Safety Board Recommendation 94-1 Implementation Plan, U. S. DOE, February 28, 1995.

2. (a) Bray, L.A.; Ryan, J.L. "Catalyzed Electrolytic Dissolution of Plutonium Dioxide," in Actinide Recovery from Waste and Low-Grade Sources. J.D. Navratil and W.W. Schulz, eds. Harwood Academic, London, 1982, pp. 129-54. (b) Bray, L.E.; Ryan, J.L.; Wheelwright, E.J. Development of the CEPOD Process for Dissolving Plutonium Oxide and Leaching Plutonium from Scrap or Waste. Pacific Northwest National Laboratory report PNL-5657, November 1985 (Unclassified Controlled Nuclear Information). (c) Wheelwright, E.J.; Bray, L.A.; Ryan, J.L. Development of the CEPOD Process for Dissolving Plutonium Oxide and Leaching Plutonium from Scrap or Wastes: 1987 Progress Report. Pacific Northwest National Laboratory report PNL-6483, March 1988 (Unclassified Controlled Nuclear Information). (d) Wheelwright, E.J.; Bray, L.A.; Bryan, G.H.; Kurath, D.E.; Ryan, J.L.; Surma, J.E. Kilogram-Scale Demonstration of Plutonium Recovery from Plant Residues Using a CEPOD II Dissolver, Anion Exchange, Oxalate Precipitation, and Calcination to Oxide. Pacific Northwest National Laboratory report PNL-7653, April 1991 (Unclassified Controlled Nuclear Information).

3. Bourges, J; Madic, C; Koehly, G; Lecomte, M. Dissolution Of Plutonium Dioxide In Nitric Medium By Electrogenerated Silver(II). Journal Of The Less-Common Metals **1986**, 122, 303-311.

4. Stumm, W. *Chemistry of the Solid-Water Interface* ; John Wiley and Sons: New York, NY, 1992.

5. Van Olphen, H. and Fripiat J. J. "Data Handbook for Clay Materials and Other Non-metallic Minerals." Pergamon Press, 1979.

6. (a) Zachara J. M. and McKinley J. P., *Aquatic Chem.* **55**, 250 (1993). (b) McKinley J.P., Zachara J.M., Smith S.C., and Turner G.D., *Clays Clay Min* **43** 586 (1995). (c)

Turner, G. D., Zachara, J. M., McKinley, J. P., and Smith, S. C., *Geochim. Cosmochim. Acta* **60**, 3399 (1996).

7. Morris, D.E. ; Chisholm-Brause, C.J. ; Barr, M.E.; Conradson , S.D.; Eller, P.G. *Geochim. Cosmochim. Acta* **1994**, 58, 3613-23.

8. Behrens , R.G.; Buck, E.C. ; Dietz, N.L.; Bates, J.K.; VanDeventer , E.; Chaiko, D.J. Characterization of Plutonium-Bearing Wastes by Chemical Analysis and Analytical Electron Microscopy. Argonne National Laboratory report ANL-95/35, September 1995.

9. *Lanthanide Probes in Life, Chemical and Earth Sciences* ; Bunzli, J.-C.G.; Choppin, G.R., Eds.; Elsevier: Amsterdam, 1989.

10. Bunzli, J.-C.G. In *Lanthanide Probes in Life, Chemical and Earth Sciences* ; Bunzli, J.-C.G.; Choppin, G.R., Eds.; Elsevier: Amsterdam, 1989; pp 219-94.

11. Horrocks, W.D., Jr.; Sudnick, D.R. *J. Am. Chem. Soc.* **1979**, 101, 334-40.

12. Kimura, T.; Choppin, G.R. *J. Alloys Compounds* **1994**, 213/214, 313-17.

13. Amadelli, R.; Maldotti, A.; Sostero, S.; Carassiti, V. *J. Chem. Soc. Faraday Trans.* **1991**, 87, 3267-73.

14. O'Day, P.A.; Chisholm-Brause, C.J.; Towle, S.N.; Parks, G.A.; Brown, Jr., G.E.. *Geochim. Cosmochim. Acta* **1996**, 60, 2515-32.

15. Papelis, C., Hayes, K. F., and Leckie, J. O., "HYDRAQL: A program for the computation of chemical equilibrium composition of aqueous batch systems including surface-complexation modeling of ion adsorption at the oxide/solution interface" , Stanford University Technical Report No. 306, 1988.

16. Grenthe, I. *Chemical Thermodynamics of Uranium*; North-Holland: New York, NY, 1992.

17. Brown, Jr., G. E.; Henrich, V.E.; Casey, W.H.; Clark, D.L.; Eggleston, C.; Felmy, A.; Goodman, D.W.; Gratzel, M.; Maciel, G.; McCarthy, M.I.; Nealson, K.H.; Sverjensky, D.A.; Toney, M.F.; Zachara, J.M. *Chem. Rev.* **1999**, 99, 77-174.

18. Kosmulski, M. *J. Colloid Interface Sci.* **1997**, 195, 395-403.

19. Rabung, T.; Geckeis, H.; Kim, J .-I.; Beck, H.P. *J. Colloid Interace Sci.* **1998**, 208, 153-61.

20. Lieser, K.H.; Quandt-Klenk, S.; Thybusch, B. *Radiochim. Acta* **1992**, 57, 45-50.

21. McKinley, J.P.; Zachara, J.M.; Smith, S.C.; Turner, G.D. *Clays Clay Minerals* **1995**, 43, 586-98.

22. Glinka, Y.D.; Jaroniec, M.; Rozenbaum, V.M. *J. Colloid Interface Sci.* **1997**, 194, 455-69.

23. Lieser, K.H.; Thybusch, B. *Fresenius Z Anal. Chem.* **1988**, 332, 351-7.

24. Moulin, C.; Wei, J.; Van Iseghem, P.; Laszak, I.; Plancque, G.; Moulin, V. *Anal. Chim. Acta* **1999**, 396, 253-61.

25. Kato, Y.; Meinrath, G.; Kimura, T.; Yoshida, Z. *Radiochim. Acta* **1994**, 64, 107-111.

26. Moulin, C.; Laszak, I.; Moulin, V.; Tondre, C. *Appl. Spectros.* **1998**, 52, 528-35.

27. Morris, D.E.; Allen, P.G.; Berg, J.M.; Chisholm-Brause, C.J.; Conradson, S.D.; Donohoe, R.J.; Hess, N.J.; Musgrave, J.A.; Tait, C.D. *Env. Sci. Tech.***1996**, 30, 2322-31.

28. Chisholm-Brause, C. J.; Berg, J. M.; Matzner, R. M.; Morris, D. E. *J. Colloid Interface Sci.* **2001**, 233, 38-49.

29. Glinka, Y.D.; Krak, T.B. *Fresenius J. Anal. Chem.* **1996**, 355, 647-50.

30. Waite, T.D.; Davis, J.A.; Payne, T.E.; Waychunas, G.A.; Xu, N. *Geochim. Cosmochim. Acta* **1994**, 58, 5465-78.

31. Morris, D. E.; Hobart, D. E.; Palmer, P. D.; Haire, R. G.; Peterson, J. R. *Radiochim. Acta* **1990**, 49, 125.

32. Docrat, T. I.; Mosselmans, J. F. W.; Charnock, J. M.; Whiteley, M. W.; Collison, D.; Livens, F. R.; Jones, C.; Edmiston, M. J. *Inorg. Chem.* **1999**, 38, 1879-82.1999.